

An Eight Loop Amplitude via Antipodal Duality

Lance J. Dixon¹ and Yu-Ting Liu¹

¹ *SLAC National Accelerator Laboratory, Stanford University, Stanford, CA 94309, USA*

E-mail: lance@slac.stanford.edu, aytliu@stanford.edu

ABSTRACT: We compute the six-particle maximally-helicity-violating (MHV) amplitude in planar $\mathcal{N} = 4$ super-Yang-Mills theory at eight loops, using antipodal duality and the recently computed eight-loop three-point form factor for the chiral stress energy tensor multiplet. Antipodal duality maps the form factor symbol to the amplitude symbol on a two-dimensional parity-preserving surface in the three-dimensional amplitude kinematics. There are remarkably few ambiguities in lifting from two to three dimensions, nor in promoting the symbol to a function. The amplitude passes many tests, including near-collinear, multi-Regge, factorization, self-crossing and origin limits. These checks also constitute a validation of antipodal duality at eight loops.

Contents

1	Introduction	2
2	Hexagon and form-factor function lightning review	6
3	Flipping the symbol on $\Delta = 0$	11
4	Lifting the symbol off $\Delta = 0$	14
5	The full function	15
5.1	At quintuple level	16
5.2	Constants beyond weight 11	17
6	Checks	18
6.1	Self-crossing limit	18
6.2	Factorization limit	20
6.3	Near-collinear (OPE) limit	23
6.4	Multi-Regge kinematics	24
7	Multiple final entry relations	26
7.1	MHV single final entries	26
7.2	MHV double final entries	26
7.3	MHV triple final entries	28
8	Parity decomposition of amplitude coproducts and locking	29
9	Amplitudes and multiple coproducts at $(1, 1, 1)$	31
9.1	Coaction principle at $(1, 1, 1)$	31
9.2	Amplitude at $(1, 1, 1)$	35
9.3	Amplitude coproducts at $(1, 1, 1)$	36
10	Weight 16 Z functions	38
10.1	Behavior at $(1, 0, 0)$	39
10.2	Behavior at the origin	40
10.3	Fixing the last weight 11 constants	40
11	The lines $(\hat{u}, \hat{u}, 1)$ and $(\hat{u}, 1, 1)$	41
12	Conclusions	44

1 Introduction

Perturbative scattering amplitudes in gauge theory lead to notoriously complicated functions of the kinematical variables, especially beyond one loop. On the other hand, there are a few examples where the functions can be expressed in terms of multiple polylogarithms (MPLs) [1–6], with a fixed symbol alphabet [7], giving hope that the all-orders behavior can be elucidated for generic kinematics. In particular, in planar $\mathcal{N} = 4$ super-Yang-Mills theory (SYM), thanks to dual conformal symmetry [8–12], the first nontrivial scattering amplitudes are for six particles, and depend on three dual conformal cross ratios [13–16]. The L -loop amplitudes are weight $2L$ polylogarithmic functions, which have symbols with words of length $2L$, whose letters in this case are drawn from a nine-letter alphabet [7]. This symbol alphabet is associated with a cluster algebra for the Grassmannian $\text{Gr}(4, 6)$ with Dynkin label A_3 [17, 18]. The hexagon alphabet describes both maximally helicity violating (MHV) and next-to-MHV (NMHV) six-particle scattering amplitudes, which can be bootstrapped to seven loops [19–28]. One also uses branch-cut information in the guise of first-entry conditions [29] and extended Steinmann relations [26, 30–32], or equivalently cluster adjacency [33, 34]. A basis of hexagon functions obeying these constraints has been constructed through weight 11 [26, 31]. Boundary conditions, as well as cross-checks, for the hexagon amplitude bootstrap come from the near-collinear limit, which corresponds to an operator product expansion (OPE) [29, 35–38] of the dual light-like closed polygonal Wilson loop [11, 13, 14, 39–45].

More recently, an even simpler quantity has been bootstrapped one loop further, to eight loops [46, 47]. That quantity is the three-particle (MHV) form factor for the chiral stress tensor operator multiplet, computed earlier through two loops [48, 49]. It depends on only two dimensionless variables and its symbol alphabet has only six letters [46, 49]. The boundary conditions for this bootstrap are provided by the recently-developed Form Factor OPE (FFOPE) [50–52].

Quite remarkably, the MHV six-particle amplitude and the three-particle form factor are antipodally dual to each other [53], which means that their symbols are precisely written backwards from each other, loop order by loop order. The duality has been verified through seven loops, because the MHV six-particle amplitude was only known through that order. The duality also involves a kinematic map, from the two-dimensional form factor kinematics into a two-dimensional parity-preserving slice of the three-dimensional amplitude kinematics.

More recently, antipodal duality has been understood to follow from a particular limit of an antipodal *self*-duality discovered for the *four*-particle MHV form factor at two loops [54]. The double collinear limit of the four-particle form factor (remainder) goes smoothly into the three-particle form factor remainder, while the triple collinear limit becomes the MHV six-particle amplitude remainder function. (The triple-collinear behavior follows from the universality of factorization limits and dual conformal invariance [13], and it can also be understood from the FFOPE [50, 54].) The four-particle form factor antipodal self-dual kinematic map neatly maps the double and triple collinear limits into each other, which means that its antipodal self-duality *subsumes* the earlier “6–3” antipodal duality. Of course,

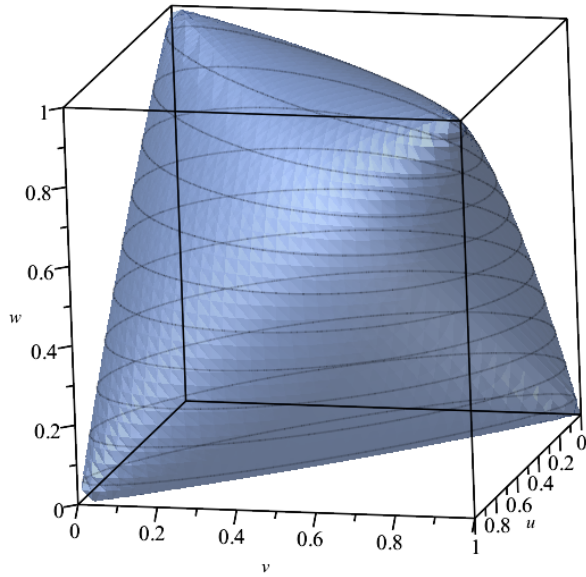


Figure 1: The surface $\Delta = 0$ inside the unit cube $0 < \hat{u}, \hat{v}, \hat{w} < 1$.

antipodal self-duality is only directly established to two loops (with three loops to appear [55]), while the 6–3 duality has been verified to seven loops.

The purpose of this paper is to exploit the 6–3 duality, and the knowledge of the eight-loop form factor [47], in order to compute the eight-loop MHV six-particle amplitude. The general idea is that applying antipodal duality to the eight-loop form factor determines the symbol of the eight-loop amplitude on the two-dimensional parity-preserving slice, and this symbol constitutes a very strong boundary condition on the full three-variable answer; there are almost no ambiguities in lifting from two to three dimensions. The power of this method suggests that it may be possible, more broadly, to bootstrap amplitudes and form factors on simpler subspaces as intermediate steps, before lifting them up to their full dimensionality.

Here we briefly outline the different steps in our computation; in the remaining sections of the paper we provide more detail and characterize the result. The first step in the computation is to apply the 6–3 kinematic map, which is a simple substitution, and then reverse the ordering of the entries in the symbol, which is computationally nontrivial, because the fully expanded symbol has over 1.67 billion terms. Because of its large size, we generally encode the symbol information in a nested format, which is organized by declaring how the derivatives of functions are related to lower-weight functions. Reversing the symbol requires undoing the nesting, but it does not need to be all undone at once; one can take advantage of initial and final-entry relations to make the computation easier.

The reversed symbol can be written using the hexagon-function basis constructed through weight 11 [26, 31]. Because the eight-loop amplitude has weight 16, this means that we express it in terms of its fifth derivatives, or more precisely, its $\{11, 1, 1, 1, 1, 1\}$ coproducts. At this

point, we know the symbol of the MHV amplitude on the two-dimensional parity-preserving surface. The next task is to lift it off that surface into the full three-dimensional bulk kinematics, which is parametrized by three dual-conformally invariant cross ratios, $(\hat{u}, \hat{v}, \hat{w})$.¹ The nine-letter hexagon alphabet is $\{\hat{u}, \hat{v}, \hat{w}, 1 - \hat{u}, 1 - \hat{v}, 1 - \hat{w}, y_u, y_v, y_w\}$. The parity-preserving surface is $\Delta(\hat{u}, \hat{v}, \hat{w}) = 0$, where $\Delta(\hat{u}, \hat{v}, \hat{w}) = (1 - \hat{u} - \hat{v} - \hat{w})^2 - 4\hat{u}\hat{v}\hat{w}$. The portion of this surface that lies within the unit cube $0 < \hat{u}, \hat{v}, \hat{w} < 1$ is shown in figure 1. On this surface, $y_u = y_v = y_w = 1$. Hence the symbol on the parity-preserving surface has only six letters, $\{\hat{u}, \hat{v}, \hat{w}, 1 - \hat{u}, 1 - \hat{v}, 1 - \hat{w}\}$, and the lifting task is to supply the dependence on the three additional parity-odd letters, $\{y_u, y_v, y_w\}$.

An important question is: How well-defined is the lifting task? How many free parameters are left after constraining the symbol to a definite value on the parity-preserving surface? That is, suppose a parity-even hexagon-function symbol is constrained to vanish on $\Delta = 0$; how many independent functions satisfy this constraint? Remarkably, through weight 10, the answer is zero — the amplitude’s symbol is fixed *uniquely* by the antipodal information! At 6 and 7 loops (weights 12 and 14, respectively), there are 1 and 3 such functions. Some of these function were encountered in ref. [26], and called Z and \tilde{Z} . They were encountered as ambiguities at a certain stage of the traditional bootstrap procedure, because they vanish in the near-collinear, or OPE limit at the level of one flux-tube excitation ($\mathcal{O}(\sqrt{\hat{v}}) = \mathcal{O}(\hat{T}^1)$ as $\hat{v} = \hat{T}^2/(1 + \hat{T}^2) \rightarrow 0$, where \hat{T} is a variable in the OPE parametrization [36]). The reason for the rapid vanishing of these functions in this limit was traced to the vanishing of their parity-even first coproducts, $Z^{u_i} = Z^{1-u_i} = \tilde{Z}^{u_i} = \tilde{Z}^{1-u_i} = 0$. Because only the parity-odd first coproducts, Z^{y_i} and \tilde{Z}^{y_i} , are nonvanishing, their symbol’s last-entry is always a y_i , and therefore their symbol vanishes on the $\Delta = 0$ surface.

Dihedral symmetry was also applied in ref. [26]; when one relaxes that constraint, one still finds only 1 function (Z) at weight 12, but there is a triplet of functions at weight 14. The cyclically invariant sum of the three functions is the \tilde{Z} function of ref. [26]. In the present case, we need to determine how many such functions there are at weight 16. The answer is 9. After imposing dihedral invariance, 3 functions are left. We could impose the OPE constraints to further trim this space, but at symbol level, since they all vanish at $\mathcal{O}(\hat{T}^1)$, it would require going to two flux-tube excitations, $\mathcal{O}(\hat{T}^2)$, which is computationally difficult. It is simpler to go to the hexagon origin, the limit $(\hat{u}, \hat{v}, \hat{w}) \rightarrow (0, 0, 0)$, where the behavior is now predicted to all orders [56, 57]. At symbol level, the coefficients of 2 of the 3 remaining functions can be fixed at the origin, but one linear combination vanishes there. Fortunately, at function level, the remaining ambiguity function does not actually vanish at the origin, and so the remaining symbol-level parameter can be fixed in the process of lifting the bulk symbol to a complete function.

There are also a few function-level ambiguities to fix at this stage. We use a small amount of OPE data to do so; just the first term in the series expansion of the one flux-tube OPE

¹We put hats on the cross ratios in order to distinguish them from similar ratios appearing in the three-particle form factor.

data is enough, thanks to the power of symbol-level antipodal duality.

After fully fixing the eight-loop result, we impose a number of cross-checks on it, including the full one flux-tube OPE behavior, and the multi-Regge limit [58]. We also check predictions of antipodal duality that go beyond the symbol [53]. On the line $(\hat{u}, \hat{v}, \hat{w}) = (\hat{u}, \hat{u}, 1)$, the amplitude collapses to harmonic polylogarithms (HPLs) [4]. Antipodal duality predicts [53] all terms that do not have an explicit π in them, including beyond-the-symbol terms proportional to odd Riemann zeta values, and multiple zeta values (MZVs). All the predictions of antipodal duality work perfectly. In summary, although we used antipodal duality at symbol level to construct the result, its beyond-the-symbol consequences are now tested at eight loops.

We plot the eight-loop result on a couple of lines. We also describe what we can learn about the MHV amplitude’s multi-final entry relations at eight loops. We provide the values of these multi-final entries at the standard hexagon-function base-point $(\hat{u}, \hat{v}, \hat{w}) = (1, 1, 1)$, where we find that remarkably few are linearly independent, and where we can test the coaction principle (also known as Cosmic Galois invariance) as in ref. [31]. We are also able to use consistency of the eight-loop amplitude, and of the $\Delta = 0$ ambiguity functions, to fix the final six remaining constants of integration in the weight 11 hexagon function space, which could not be fixed at seven loops [31].

This paper is organized as follows. In section 2 we provide a lightning review of hexagon functions and the coproduct formalism. In section 3 we explain how to flip a weight 16, 1.67 billion term symbol. Section 4 describes how we lift the symbol off of the parity-preserving slice, up to a one-parameter ambiguity. In section 5 we fix that ambiguity, as well as all beyond-the-symbol ambiguities, using various boundary conditions. Section 6 describes how the eight-loop amplitude passes numerous checks involving four different kinematic limits. In section 7 we describe empirical linear relations among the multiple final entries of the amplitude, which we expect to hold to all loop orders. Section 8 describes how a few of the beyond-the-symbol hexagon functions are not needed when the amplitude is optimally (cosmically) normalized, because they always appear “locked” to other functions. In section 9 we study the values of the amplitudes and their multiple coproducts at the hexagon-function base point $(1, 1, 1)$, and test the coaction principle there. Section 10 describes a set of parity-even “ Z ” functions, which vanish on the entire parity-preserving surface, but not off it; they are the essential ambiguities in lifting off the surface. In section 11 we provide numerical results at $(1, 1, 1)$ and along a pair of lines that intersect at that point. Finally, in section 12 we present our conclusions.

A number of results are best presented as computer-readable ancillary files. We provide the following such files along with this paper: `MHV8quintuples.txt` gives the weight 11 quintuple coproducts of the eight-loop MHV amplitude in terms of the hexagon function basis; `EZMHVcoproducts111.txt` provides the constant values of the eight-loop coproducts with higher weights (12 to 16) at $(1, 1, 1)$, along with lower-loop values; `RLncy.txt` provides the near-collinear (OPE) limits of the remainder function; `RLncyser.txt` gives a further series expansion in S ; `MRKSigma.txt` provides the perturbative expansion of the multi-Regge limit through eight loops; `EZsmallercoproductspace.txt` gives a reduced space of hexagon

functions revealed by the amplitudes' coproducts; `ftoMZV16.txt` converts between two representations of MZVs; `Zorigin.txt` gives the values of the weight 16 Z functions at the origin; and `EZMHVg_uu1_lin.txt` and `EZMHVg_u11_lin.txt` give the values of the MHV amplitude on the lines $(\hat{u}, \hat{u}, 1)$ and $(\hat{u}, 1, 1)$, respectively. All these files are hosted at [59].

2 Hexagon and form-factor function lightning review

In this section we provide a lightning review of the space of hexagon functions, which describes six-particle amplitudes in planar $\mathcal{N} = 4$ SYM. For further details, the reader is referred to refs. [21, 26, 27, 31]. Then we briefly describe the space of form-factor functions; see refs. [46, 47] for further details. We also introduce a new amplitude normalization factor [56], and review the antipodal map between the three-particle form factor and the MHV amplitude.

The coefficients in the perturbative expansion of six-point scattering amplitudes in planar $\mathcal{N} = 4$ SYM are hexagon functions, a particular case of generalized polylogarithms, or iterated integrals over logarithmic kernels. Generalized polylogarithms can be defined iteratively by

$$G_{a_1, \dots, a_n}(z) = \int_0^z \frac{dt}{t - a_1} G_{a_2, \dots, a_n}(t), \quad G_{\underbrace{0, \dots, 0}_p}(z) = \frac{\ln^p z}{p!}, \quad (2.1)$$

with $G(z) \equiv 1$. The *weight* of $G_{a_1, \dots, a_n}(z)$ is the number of integrations n .

The differential of any such function F has the form

$$dF = \sum_{\phi \in \mathcal{L}} F^\phi d \ln \phi, \quad (2.2)$$

where the *symbol letters* ϕ belong to the *alphabet* \mathcal{L} , and the *first coproduct* F^ϕ is also an iterated integral with weight one lower than F . For hexagon functions, the alphabet has nine letters. The original alphabet for the hexagon function bootstrap was [19]

$$\mathcal{L}_{\text{hex}}^u = \{\hat{u}, \hat{v}, \hat{w}, 1 - \hat{u}, 1 - \hat{v}, 1 - \hat{w}, y_u, y_v, y_w\}, \quad (2.3)$$

where the dual conformal cross ratios are

$$\hat{u} = \frac{x_{13}^2 x_{46}^2}{x_{14}^2 x_{36}^2} = \frac{s_{12} s_{45}}{s_{123} s_{345}}, \quad \hat{v} = \frac{x_{24}^2 x_{51}^2}{x_{25}^2 x_{41}^2}, \quad \hat{w} = \frac{x_{35}^2 x_{62}^2}{x_{36}^2 x_{52}^2}. \quad (2.4)$$

Here we will mainly (but not always) use the equivalent alphabet [25],

$$\mathcal{L}_{\text{hex}}^a = \{\hat{a}, \hat{b}, \hat{c}, \hat{d}, \hat{e}, \hat{f}, y_u, y_v, y_w\}, \quad (2.5)$$

where

$$\hat{a} = \frac{\hat{u}}{\hat{v}\hat{w}}, \quad \hat{b} = \frac{\hat{v}}{\hat{w}\hat{u}}, \quad \hat{c} = \frac{\hat{w}}{\hat{u}\hat{v}}, \quad \hat{d} = \frac{1 - \hat{u}}{\hat{u}}, \quad \hat{e} = \frac{1 - \hat{v}}{\hat{v}}, \quad \hat{f} = \frac{1 - \hat{w}}{\hat{w}}. \quad (2.6)$$

and $\hat{u}, \hat{v}, \hat{w}$ are the usual dual conformal cross ratios. We put hats on them to distinguish them from the ordinary ratios u, v, w for the form factor.

The parity-odd letters,

$$y_u = \frac{\hat{u} - z_+}{\hat{u} - z_-}, \quad y_v = \frac{\hat{v} - z_+}{\hat{v} - z_-}, \quad y_w = \frac{\hat{w} - z_+}{\hat{w} - z_-}, \quad (2.7)$$

are defined in terms of

$$z_{\pm} = \frac{1}{2} \left[-1 + \hat{u} + \hat{v} + \hat{w} \pm \sqrt{\Delta} \right], \quad \Delta = (1 - \hat{u} - \hat{v} - \hat{w})^2 - 4\hat{u}\hat{v}\hat{w}. \quad (2.8)$$

The dihedral symmetry group D_6 contains an S_3 permuting $(\hat{u}_1, \hat{u}_2, \hat{u}_3) \equiv (\hat{u}, \hat{v}, \hat{w})$ and $(y_1, y_2, y_3) \equiv (y_u, y_v, y_w)$. In terms of the alphabet $\mathcal{L}_{\text{hex}}^a$, the S_3 is generated by:

$$\text{cycle: } \hat{a} \rightarrow \hat{b} \rightarrow \hat{c} \rightarrow \hat{a}, \quad \hat{d} \rightarrow \hat{e} \rightarrow \hat{f} \rightarrow \hat{d}, \quad y_u \rightarrow 1/y_v \rightarrow y_w \rightarrow 1/y_u, \quad (2.9)$$

$$\text{flip: } \hat{a} \leftrightarrow \hat{b}, \quad \hat{d} \leftrightarrow \hat{e}, \quad y_u \leftrightarrow y_v, \quad (2.10)$$

There is also the parity transformation, whose only effect is to invert the parity-odd letters, $y_i \leftrightarrow 1/y_i$. On the parity-even surface,

$$\Delta(\hat{u}, \hat{v}, \hat{w}) = 0, \quad (2.11)$$

all the $y_i \rightarrow 1$, which means that they drop out of the symbol, reducing it to six letters, $\{\hat{a}, \hat{b}, \hat{c}, \hat{d}, \hat{e}, \hat{f}\}$, the same number as for the three-particle form factor [46, 47, 49].

For the form factor for three massless particles, momentum conservation reads $p_1 + p_2 + p_3 = -q$, where q is the operator momentum. Squaring this relation and using $p_i^2 = 0$, we have

$$q^2 = s_{123} = s_{12} + s_{23} + s_{31}, \quad (2.12)$$

where $s_{ij} = (p_i + p_j)^2$. The dimensionless ratios,

$$u = \frac{s_{12}}{q^2}, \quad v = \frac{s_{23}}{q^2}, \quad w = \frac{s_{31}}{q^2}, \quad (2.13)$$

obey

$$u + v + w = 1, \quad (2.14)$$

as a consequence of eq. (2.12).

The form-factor symbol alphabet is [46, 47, 49]

$$\mathcal{L}_{\mathbb{F}3}^a = \{a, b, c, d, e, f\}, \quad (2.15)$$

where

$$a = \frac{u}{vw}, \quad b = \frac{v}{wu}, \quad c = \frac{w}{uv}, \quad d = \frac{1-u}{u}, \quad e = \frac{1-v}{v}, \quad f = \frac{1-w}{w}. \quad (2.16)$$

There is a dihedral symmetry S_3 generated by

$$\text{cycle: } a \rightarrow b \rightarrow c \rightarrow a, \quad d \rightarrow e \rightarrow f \rightarrow d, \quad (2.17)$$

$$\text{flip: } a \leftrightarrow b, \quad d \leftrightarrow e. \quad (2.18)$$

Generalized polylogarithms are naturally equipped with a coaction Δ [7, 60–64] which maps weight n functions to (sums of) products of functions (roughly) of weight $(n-p)$ and p , for any integer p between 0 and n . The $p = 1$ case, or $\{n-1, 1\}$ component of the coaction, is equivalent to the total differential (2.2):

$$\Delta_{n-1,1}(F) = \sum_{\phi \in \mathcal{L}} F^{\phi} \otimes \ln \phi. \quad (2.19)$$

The map $\Delta_{\bullet,1}$ can be applied iteratively to each F^{ϕ} , leading to the *second coproducts* $F^{\phi',\phi}$, etc. Continuing on n times, the weight n polylogarithms entering F are mapped to n -fold tensor products of logarithms, the *symbol* of F [7]. The arguments of the logarithms are the symbol alphabet.

The perturbative coefficients of the six-point amplitude at L loops can be expressed in terms of weight $2L$ polylogarithms. However, it is not practical to write out such an expression explicitly at high loop orders, because the number of G functions required grows roughly by a factor of 5 at each weight, so the seven loop results might require around a billion terms. Instead, we use a nested description, the coproduct formalism [21, 31]. This formalism describes the first derivative of any function F (which might be an amplitude or a basis function) in terms of its first coproducts F^{ϕ} . Those functions are in turn described by their first coproducts, and so on down to logarithms. Let $F_{i_n}^{(n)}$, $i_n = 1, 2, \dots, d_n$ denote a basis for the weight n part of the hexagon function space \mathcal{H}^{hex} , which has dimension d_n . Also give the letters a discrete label k , so that $\phi_k \in \mathcal{L}$. Then the coproducts are described by a \mathbb{Q} -valued three-index tensor T , with dimension $d_n \times d_{n-1} \times |\mathcal{L}|$,

$$\Delta_{n-1,1} F_{i_n}^{(n)} = \sum_{i_{n-1}, k} T_{i_n, i_{n-1}}^k F_{i_{n-1}}^{(n-1)} \otimes \ln \phi_k, \quad (2.20)$$

where $|\mathcal{L}_{\text{hex}}| = 9$ and $|\mathcal{L}_{\text{F3}}| = 6$.

We begin the construction of \mathcal{H}^{hex} at weight 1 by imposing the branch-cut conditions, which requires that the first letter in the symbol is drawn from $\{\hat{u}, \hat{v}, \hat{w}\}$, or equivalently $\{\hat{a}, \hat{b}, \hat{c}\}$. In other words,

$$\mathcal{H}_1^{\text{hex}} = \{\ln \hat{a}, \ln \hat{b}, \ln \hat{c}\}. \quad (2.21)$$

In constructing $\mathcal{H}_n^{\text{hex}}$ at higher weights n , we impose integrability, $d^2 F = 0$, as well as the extended Steinmann relations [25, 31], that \hat{a} never appears adjacent to \hat{b} ,

$$\dots \otimes \hat{a} \otimes \hat{b} \otimes \dots, \quad (2.22)$$

plus the five other conditions generated by dihedral symmetry.

In terms of double coproducts of functions F , the extended Steinmann conditions are

$$F^{\hat{a}, \hat{b}} = F^{\hat{b}, \hat{c}} = F^{\hat{c}, \hat{a}} = F^{\hat{b}, \hat{a}} = F^{\hat{c}, \hat{b}} = F^{\hat{a}, \hat{c}} = 0. \quad (2.23)$$

We impose these conditions along with integrability and the first-entry condition. Together, these conditions lead to 41 relations among the $9 \times 9 = 81$ adjacent pairs of letters, or

equivalently 40 independent pairs of adjacent entries [26, 30, 31], which also corresponds to the A_3 cluster adjacency conditions [33, 34]. Included in these relations are the non-adjacency of symbol letters \hat{a} and \hat{d} , plus four other relations generated by dihedral symmetry:

$$F^{\hat{a},\hat{d}} = F^{\hat{b},\hat{e}} = F^{\hat{c},\hat{f}} = F^{\hat{d},\hat{a}} = F^{\hat{e},\hat{b}} = F^{\hat{f},\hat{c}} = 0. \quad (2.24)$$

In addition, we only include constants (zeta values) as independent functions when the amplitudes' coproducts dictate their presence. As in refs. [25, 31], this means that the only independent zeta-valued constants are $\zeta_4, \zeta_6, \zeta_8, \zeta_{10}$, etc.

In some cases we use the old alphabet $\mathcal{L}_{\text{hex}}^u$, for example to describe the multi-final entry relations in section 7. One can convert between alphabets using the following relations between coproducts:

$$\begin{aligned} F^{\hat{u}} &= F^{\hat{a}} - F^{\hat{b}} - F^{\hat{c}} - F^{\hat{d}}, \\ F^{\hat{v}} &= -F^{\hat{a}} + F^{\hat{b}} - F^{\hat{c}} - F^{\hat{e}}, \\ F^{\hat{w}} &= -F^{\hat{a}} - F^{\hat{b}} + F^{\hat{c}} - F^{\hat{f}}, \\ F^{1-\hat{u}} &= F^{\hat{d}}, \\ F^{1-\hat{v}} &= F^{\hat{e}}, \\ F^{1-\hat{w}} &= F^{\hat{f}}. \end{aligned} \quad (2.25)$$

Besides giving all the first derivatives of the hexagon functions through the coproduct tensors T , through weight 11, we must also specify the values of the basis functions at one point, as integration constants. For hexagon functions, we use the base point $(\hat{u}, \hat{v}, \hat{w}) = (1, 1, 1)$ in the Euclidean region. This point is dihedrally symmetric, all the functions are finite there, and they all evaluate to multiple zeta values (MZVs). The coproduct and base point data for \mathcal{H}^{hex} is complete through weight 11 (up to a few weight 11 constants n_i , which are fixed below), and it is provided in the ancillary files for refs. [26, 31], which are stored at [59].

We remark that the function-level part of the weight 11 basis in the parity-even sector is sub-optimal; the coproduct tensors contain rational numbers with large denominators in some cases. This fact means that some care has to be taken when reconstructing the rational-number coefficients of some of the basis functions, if the constraint equations are initially solved over a prime number field.

In this work, we use a new, all-orders ‘‘cosmic’’ BDS-like normalization of the MHV amplitude, inspired by the amplitude’s behavior at the origin [56],

$$\mathcal{E} = \frac{1}{\rho} \exp \left[\frac{\Gamma_{\text{cusp}}}{4} \mathcal{E}^{(1)} + \mathcal{R} \right], \quad (2.26)$$

where \mathcal{R} is the remainder function, and

$$\rho = \det(\mathbb{I} + \mathbb{K}) \exp \left[-\frac{1}{2} \zeta_2 \Gamma_{\text{cusp}} \right]. \quad (2.27)$$

Here \mathbb{K} is the semi-infinite matrix kernel of the BES equation [65], which provides the cusp anomalous dimension Γ_{cusp} to all orders in g^2 , in terms of the 1,1 matrix element of the matrix inverse,

$$\frac{\Gamma_{\text{cusp}}}{4} = g^2 \left[(\mathbb{I} + \mathbb{K})^{-1} \right]_{1,1}, \quad (2.28)$$

and \mathbb{I} is the identity matrix.

The formula (2.27) has the perturbative expansion through eight loops,

$$\begin{aligned} \rho(g^2) = & 1 - \zeta_4 g^4 + \left[\frac{50}{3} \zeta_6 + 8(\zeta_3)^2 \right] g^6 - \left[\frac{2891}{12} \zeta_8 + 160 \zeta_3 \zeta_5 \right] g^8 \\ & + \left[\frac{10265}{3} \zeta_{10} - 40 \zeta_4 (\zeta_3)^2 + 1680 \zeta_3 \zeta_7 + 912 (\zeta_5)^2 \right] g^{10} \\ & - \left[\frac{4857061891}{99504} \zeta_{12} - \frac{1600}{3} \zeta_6 (\zeta_3)^2 - 608 \zeta_4 \zeta_3 \zeta_5 + 18816 \zeta_3 \zeta_9 + 20832 \zeta_5 \zeta_7 \right] g^{12} \\ & + \left[\frac{50570065}{72} \zeta_{14} - 6370 \zeta_8 (\zeta_3)^2 - \frac{24320}{3} \zeta_6 \zeta_3 \zeta_5 - 5040 \zeta_4 \zeta_3 \zeta_7 - 2736 \zeta_4 (\zeta_5)^2 \right. \\ & \quad \left. + 221760 \zeta_3 \zeta_{11} + 247296 \zeta_5 \zeta_9 + 126240 (\zeta_7)^2 \right] g^{14} \\ & - \left[\frac{63718004141707}{6250176} \zeta_{16} - \frac{230960}{3} \zeta_{10} (\zeta_3)^2 - 98056 \zeta_8 \zeta_3 \zeta_5 - 67840 \zeta_6 \zeta_3 \zeta_7 \right. \\ & \quad \left. - 34880 \zeta_6 (\zeta_5)^2 - 45696 \zeta_4 \zeta_3 \zeta_9 - 52128 \zeta_4 \zeta_5 \zeta_7 - 320 \zeta_4 (\zeta_3)^4 \right. \\ & \quad \left. + 2718144 \zeta_3 \zeta_{13} + 3130560 \zeta_7 \zeta_9 + 3041280 \zeta_5 \zeta_{11} \right] g^{16} + \mathcal{O}(g^{18}). \end{aligned} \quad (2.29)$$

Previously, a different ‘‘cosmic’’ normalization factor ρ_{old} was used, namely eq. (2.29) of ref. [26]. It was determined by imposing the coaction principle through weight 14, and a few other constraints. It was inherently ambiguous as to the pure ζ_{2L} terms (π^{2L} terms), because they have no nontrivial terms in their coaction. Equation (2.29) of ref. [26] matches eq. (2.29) through seven loops, up to pure ζ_{2L} terms. To convert from the normalizations used in refs. [26, 31] to the new, all-orders normalization (2.27), one should multiply the old \mathcal{E} functions (and also the NMHV components E and \tilde{E}) by the factor

$$\begin{aligned} \frac{\rho_{\text{old}}}{\rho} = & 1 + \zeta_4 g^4 - \frac{50}{3} \zeta_6 g^6 + \frac{2905}{12} \zeta_8 g^8 - \frac{10375}{3} \zeta_{10} g^{10} + \frac{4937878055}{99504} \zeta_{12} g^{12} \\ & - \frac{51698725}{72} \zeta_{14} g^{14} + \mathcal{O}(g^{16}). \end{aligned} \quad (2.30)$$

The precise statement of antipodal duality between the three-particle form factor \mathcal{E}_c and the MHV six-particle amplitude \mathcal{E} on the latter’s parity-preserving surface is²

$$\mathcal{E}(\hat{u}, \hat{v}, \hat{w}) \Big|_{\Delta=0} = S(\mathcal{E}_c(u, v, w)). \quad (2.31)$$

²Note that \mathcal{E} here is called A_6 in ref. [53], and \mathcal{E}_c here is called F_3 there.

Here S is the antipode map which reverses the order of letters in every word in the symbol:

$$S(x_1 \otimes \cdots \otimes x_m) = (-1)^m x_m \otimes \cdots \otimes x_1. \quad (2.32)$$

The kinematic map in eq. (2.31) can be written as

$$\hat{u} = \frac{vw}{(1-v)(1-w)}, \quad \hat{v} = \frac{wu}{(1-w)(1-u)}, \quad \hat{w} = \frac{uv}{(1-u)(1-v)}. \quad (2.33)$$

At the level of the symbol letters, going from the form-factor to the amplitude, it acts as

$$\begin{aligned} a &\rightarrow \hat{d}, & b &\rightarrow \hat{e}, & c &\rightarrow \hat{f}, \\ d &\rightarrow \sqrt{\hat{a}}, & e &\rightarrow \sqrt{\hat{b}}, & f &\rightarrow \sqrt{\hat{c}}. \end{aligned} \quad (2.34)$$

It is easy to verify that it maps the form-factor surface $u + v + w = 1$ into the amplitude's parity-preserving surface $\Delta(\hat{u}, \hat{v}, \hat{w}) = 0$. The dihedral symmetry S_3 of the form factor, eqs. (2.17) and (2.18), maps into the dihedral symmetry $D_6/Z_2 \equiv S_3$ of the amplitude, eqs. (2.9) and (2.10). The antipode map can be defined beyond the symbol level, which will play a role in checks later in the paper. However, mathematically it is only defined modulo $i\pi$ (see e.g. ref. [66]). That is, any additive term containing a factor of $i\pi$, including all even Riemann ζ values, which are powers of π^2 , cannot be predicted at present.

3 Flipping the symbol on $\Delta = 0$

The first task in computing the eight-loop MHV six-particle amplitude $\mathcal{E}^{(8)}$ via antipodal duality is to construct its symbol on the $\Delta = 0$ surface. The starting point is the symbol of the eight-loop form-factor $\mathcal{E}_c^{(8)}$, which is provided in the ancillary file `EsymbOct8.txt` for ref. [47]. There are 279 linearly independent octuple final entries for the form factor, which can be organized into 93 three-orbits under the cyclic symmetry, and this is how the symbol is stored in `EsymbOct8.txt`. Additionally, instructions for “integrating up” the octuple representation to one based on heptuples, hexuples, etc., using the multi-final-entry relations obeyed by $\mathcal{E}_c^{(8)}$, are given in the ancillary file `Esymb.txt` for ref. [47]. See also section 4.2 of that reference for the first few multi-final entry relations. While the full symbol is too unwieldy, we choose to integrate it up to the level of the triple final entries. As mentioned in ref. [47], there are 12 independent final entries, which can be organized into 4 three-orbits under the cyclic symmetry. Here we take as representatives $\mathcal{E}_c^{f,f,f}$, $\mathcal{E}_c^{a,f,f}$, $\mathcal{E}_c^{f,a,f}$ and $\mathcal{E}_c^{a,a,f}$.³ Using the alphabet $\mathcal{L}_{\mathbb{F}_3}^a$, the respective numbers of terms in their weight 13 symbols are $n_{f,f,f} = 58,831,962$, $n_{a,f,f} = 95,178,164$, $n_{f,a,f} = 58,826,293$, and $n_{a,a,f} = 36,362,651$.

There is one other three-orbit of form-factor triple final entries, which is not linearly independent, but which is useful to construct in order to count all the terms in the symbol: $\mathcal{E}^{e,a,f} = \mathcal{E}^{f,a,f} - \mathcal{E}^{a,f,f}$, which has $n_{e,a,f} = 58,826,293$ terms in its symbol. Using the form factor's double and triple final entry relations from section 4.2 of ref. [47], as well as dihedral

³For clarity, we will drop the superscript (8) for the rest of this section, since everything is at eight loops.

symmetry, we find that the number of terms in the independent form-factor double final entries ($\mathcal{E}_c^{f,f}$ and $\mathcal{E}_c^{a,f}$) is

$$\begin{aligned} n_{f,f} &= 2n_{a,f,f} + n_{f,f,f} = 249,188,290, \\ n_{a,f} &= n_{a,a,f} + n_{e,a,f} + n_{f,a,f} = 154,015,237. \end{aligned} \quad (3.1)$$

The number of symbol terms for the one dihedrally independent single final entry (\mathcal{E}_c^f) is then

$$n_f = 2n_{a,f} + n_{f,f} = 557,218,764. \quad (3.2)$$

By cyclic symmetry, the total number of terms in the form-factor symbol is just three times this,

$$n_{F3} = 3n_f = 1,671,656,292. \quad (3.3)$$

This number will be useful as a check that we flipped the symbol properly.

On the amplitude side, we also work at the level of triple final entries. These correspond to triple initial entries on the form-factor side. We find that there are 62 independent triple final entries for the MHV amplitude. However, only 21 of them contain no y_i index and so can be obtained by flipping the form factor symbol. (These 21 no- y_i final entries are in one-to-one correspondence with the number of independent weight 3 functions in the form-factor space, see Table 2 of ref. [47].) The 21 triple final entries can be organized into 7 three-orbits under the amplitude cyclic symmetry. We take as representatives $\mathcal{E}^{\hat{c},\hat{c},\hat{d}}$, $\mathcal{E}^{\hat{b},\hat{d},\hat{d}}$, $\mathcal{E}^{\hat{d},\hat{c},\hat{d}}$, $\mathcal{E}^{\hat{e},\hat{c},\hat{d}}$, $\mathcal{E}^{\hat{d},\hat{f},\hat{d}}$, $\mathcal{E}^{\hat{f},\hat{f},\hat{d}}$ and $\mathcal{E}^{\hat{d},\hat{d},\hat{d}}$. Using the alphabet $\mathcal{L}_{\text{hex}}^a$, the respective numbers of terms in their weight 13 symbols are

$$\begin{aligned} n_{\hat{c},\hat{c},\hat{d}} &= 20,632,545, & n_{\hat{b},\hat{d},\hat{d}} &= 20,627,110, & n_{\hat{d},\hat{c},\hat{d}} &= 33,380,402, & n_{\hat{e},\hat{c},\hat{d}} &= 33,380,402, \\ n_{\hat{d},\hat{f},\hat{d}} &= 33,340,897, & n_{\hat{f},\hat{f},\hat{d}} &= 33,340,897, & n_{\hat{d},\hat{d},\hat{d}} &= 33,338,326. \end{aligned} \quad (3.4)$$

We obtained their symbols from those of $\mathcal{E}_c^{f,f,f}$, etc., by clipping off the appropriate first three entries on the form-factor side (e.g. a, f, f for $\mathcal{E}^{\hat{c},\hat{c},\hat{d}}$), and then using the form-factor triple, double and single final-entry relations to integrate up all the way to the back of the form factor (front of the amplitude, after applying the antipodal map). It is straightforward to apply S between the alphabets \mathcal{L}_{F3}^a and $\mathcal{L}_{\text{hex}}^a$ because it is a simple substitution, so that no re-factoring of the symbol is required. (Re-factoring of such large symbols can be computationally expensive.)

There are 3 other three-orbits of amplitude triple final entries which are not linearly independent, but which are useful to construct in order to re-count all the terms in the symbol: $\mathcal{E}^{\hat{e},\hat{f},\hat{d}}$ ($n_{\hat{e},\hat{f},\hat{d}} = 33,262,314$ terms), $\mathcal{E}^{\hat{e},\hat{d},\hat{d}}$ ($n_{\hat{e},\hat{d},\hat{d}} = 33,349,686$ terms), $\mathcal{E}^{\hat{b},\hat{f},\hat{d}}$ ($n_{\hat{b},\hat{f},\hat{d}} = 20,625,966$ terms). In order to count the terms in the full symbol, we first use the the triple final-entry enumeration to count the number of terms in each double final entry. Using the amplitude's double and triple final entry relations (which include $\mathcal{E}^{\hat{a},\hat{f},\hat{d}} = 0$) and dihedral symmetry, we

find that

$$\begin{aligned}
n_{\hat{c},\hat{d}} &= n_{\hat{c},\hat{c},\hat{d}} + n_{\hat{d},\hat{c},\hat{d}} + n_{\hat{e},\hat{c},\hat{d}} = 87,393,349, \\
n_{\hat{f},\hat{d}} &= n_{\hat{b},\hat{f},\hat{d}} + n_{\hat{d},\hat{f},\hat{d}} + n_{\hat{e},\hat{f},\hat{d}} + n_{\hat{f},\hat{f},\hat{d}} = 120,570,074, \\
n_{\hat{d},\hat{d}} &= 2n_{\hat{b},\hat{d},\hat{d}} + n_{\hat{d},\hat{d},\hat{d}} + 2n_{\hat{e},\hat{d},\hat{d}} = 141,291,918.
\end{aligned}
\tag{3.5}$$

Finally we count the number of terms in the one dihedrally independent single final entry ($\mathcal{E}^{\hat{d}}$):

$$n_{\hat{d}} = 2n_{\hat{c},\hat{d}} + n_{\hat{d},\hat{d}} + 2n_{\hat{f},\hat{d}} = 557,218,764. \tag{3.6}$$

The total number of terms in the eight-loop amplitude’s symbol on the parity-preserving surface is just three times this,

$$n_{\Delta=0} = 3n_{\hat{d}} = 1,671,656,292. \tag{3.7}$$

This number matches the number of terms (3.7) counted from the form-factor side, which is a very useful cross-check that we flipped the symbol correctly.

The weight 13 triple final entries still have rather unwieldy symbols, so the next step is to “re-nest” the information using the basis for the hexagon function space \mathcal{H}^{hex} . Since this basis (at least a computationally useful one) only exists through weight 11, we should organize the MHV amplitudes according to their $\{11, 1, 1, 1, 1, 1\}$ coproducts, or quintuple final entries. We start with the MHV amplitude triple final entries in the bulk. As discussed in section 7, the number of such entries has saturated by seven loops at 62, of which 31 are parity-even and 31 are parity-odd. We take the 62 MHV amplitude triple final entries, and put any of the 9 hexagon letters in front of them, in order to obtain 9×62 potential quadruple final entries. We then impose the 41 pair relations for \mathcal{H}^{hex} , acting in the 4th-3rd slots from the back. We find that there are 166 independent quadruple final entries; 84 are parity-even and 82 are parity-odd. 48 of the 166 have no y_i indices; they correspond to the 48 independent weight 4 functions in the form-factor space — see again Table 2 of ref. [47].

To get the independent quintuple final entries, we repeat the exercise: we put all 9 hexagon letters in front of the 166 independent quadruples and impose the \mathcal{H}^{hex} pair relations. We find 424 independent quintuples, 211 parity-even and 213 parity-odd. Of the 424 quintuples, 108 have no y_i indices, which matches the ‘108’ in the weight 5 column in Table 2 of ref. [47]. We place these 108 quintuples into the (symbol-level part of) the weight 11 hexagon function basis, using the above weight 13 symbols $\mathcal{E}^{\hat{c},\hat{c},\hat{d}}, \dots$

The only slight catch is that we didn’t write out the symbols for all the weight 11 functions in \mathcal{H}^{hex} , because the table would have been too large. We only did so up to weight 9. So in practice, for each of the 108 no- y_i quintuple final entries, we first generated their weight 11 symbols by clipping the appropriate pairs of entries off the back of the weight 13 symbols. Then we clipped off pairs of additional entries to get to weight 9, where we could map them into \mathcal{H}^{hex} . Then we found the unique weight 11 elements of \mathcal{H}^{hex} with those weight 9 double coproducts. These 108 weight 11 quintuple final entries are uniquely determined in the bulk of the amplitude kinematic space; that is because ambiguities in lifting off of the $\Delta = 0$ surface only begin at weight 12.

4 Lifting the symbol off $\Delta = 0$

The next step in computing the eight-loop MHV six-particle amplitude is to lift the symbol off of the $\Delta = 0$ surface, where all the $y_i = 1$, into the bulk three-dimensional kinematics. To do this, we need to determine the $424 - 108 = 316$ quintuple final entries that have one or more y_i indices. Of the 316 such quintuples, $211 - 108 = 103$ are parity-even and 213 are parity odd. The main tool for determining them is the set of 41 pair relations for the 6th-5th slots from the back. One could in principle float unknowns for all 316 quintuple final entries at once, and use the pair relations to relate them to the coproducts of the 108 known quintuples. At weight 11 and at symbol level, there are 1503 parity-even and 382 parity-odd functions. The total number of unknowns would be $103 \times 1503 + 213 \otimes 382 = 236,175$, which is a pretty large linear system to solve.

In order to reduce the number of unknowns encountered at a single stage, we solve for the missing quintuples in layers, organized by the number and location of the y_i entries, instead of solving for all of them at once. The 108 known quintuples have the generic form $\mathcal{E}^{e_{i_1}, e_{i_2}, e_{i_3}, e_{i_4}, e_{i_5}}$, where e_i stands for any of the 6 parity-even hexagon letters. Suppose we try to solve first for quintuples of the form $\mathcal{E}^{y_{j_1}, e_{i_1}, e_{i_2}, e_{i_3}, e_{i_4}}$, with a y in the first of the five slots. We call these “no- y quads”. For example, a pair relation of the form $F^{\hat{u}, y_u} = F^{y_u, \hat{u}}$, applied in the 6th-5th slots from the back, allows us to relate an even coproduct of a $\mathcal{E}^{y_{j_1}, e_{i_1}, e_{i_2}, e_{i_3}, e_{i_4}}$ to an odd coproduct of one of the known $\mathcal{E}^{e_{i_1}, e_{i_2}, e_{i_3}, e_{i_4}, e_{i_5}}$. After combining the no- y quads with the known 108 quintuples, and applying all of the quintuple relations, we find that there are 99 more independent quintuples. We can determine them one at a time using 6th-5th slot pair relations, so we never need more than 1503 unknowns, making the relations easy to solve. The no- y quads have weight 12, so we can expect some unknown constants to crop up, which are related to the weight 12 function Z discussed in the introduction. Using dihedral symmetry, we found just 11 constants in all, at quad level. (These constant parameters multiply weight 12 symbols, and are unrelated to zeta-valued constants.)

Next we add quintuples that come from the “no- y triples”, i.e. of the form $\mathcal{E}^{e_{i_0}, y_{j_1}, e_{i_1}, e_{i_2}, e_{i_3}}$ or $\mathcal{E}^{y_{j_0}, y_{j_1}, e_{i_1}, e_{i_2}, e_{i_3}}$. There are 69 additional quintuples of this type, and they are associated with 21 no- y triples. Determining them is also not a major computation. When we solve for the weight 13 triples, we also determine all but 2 of the 11 constants that were required at quad level, and no additional triple-level constants have to be introduced. So far we have fixed $108 + 99 + 69 = 276$ of the 424 quintuples, up to these 2 free parameters.

Next we solve for the “no- y doubles”, which correspond to 54 additional quintuples, or $276 + 54 = 330$ in all. Up to cyclic permutations, their last two entries are $\{\hat{c}, \hat{d}\}$, $\{\hat{d}, \hat{d}\}$, and $\{\hat{f}, \hat{d}\}$. We have to introduce $1 \times 1503 + 3 \times 382 = 2649$ unknowns for 4 different quintuples associated with $\{\hat{f}, \hat{d}\}$, $4 \times 1503 + 10 \times 382 = 9832$ unknowns for $\{\hat{d}, \hat{d}\}$, and $4 \times 1503 + 9 \times 382 = 9450$ unknowns for $\{\hat{c}, \hat{d}\}$. These equations could all be solved over the rational numbers, up to just 3 undetermined constants.

Similarly, the “no- y singles” correspond to 24 additional quintuples, or 354 in all. Up to cyclic permutations, their last entry is \hat{d} , and we have to introduce $9 \times 1503 + 6 \times 382 = 15,819$

unknown parameters, which is still feasible to solve over the rationals. The combined solution, for everything but the y_i final entries, has *no* undetermined constants at symbol level.

The final step in lifting the symbol to the bulk is to determine the additional quintuples associated with an odd final entry, which by cyclic symmetry can be taken to be y_u . There are still $424 - 354 = 70$ such quintuples left to fix; 28 are parity-even and 42 are parity-odd. The corresponding number of unknown parameters is $28 \times 1503 + 42 \times 382 = 58,128$. This linear system is large enough that we had to first solve it over prime number fields \mathbb{Z}_p for a few different primes p , and then reconstruct the rational number solution, along the lines of e.g. refs. [67, 68]. We obtained a three-parameter, dihedrally symmetric, solution space. (Later we relaxed the condition of dihedral symmetry on the homogeneous part of the solution, i.e. functions F satisfying $F^{e_i} = 0$ for all parity-even letters e_i , and we found 9 unfixed parameters, corresponding to a 9-dimensional space of ambiguities for lifting weight 16 symbols off of the surface $\Delta = 0$.)

Next we evaluated the 3-parameter solution (still over the primes) at the kinematical origin, $(\hat{u}, \hat{v}, \hat{w}) \rightarrow (0, 0, 0)$. The remainder function \mathcal{R} in eq. (2.26) is quadratic in $\ln \hat{u}_i$ at the origin, with zeta-valued coefficients [56]; thus its symbol vanishes there, up to power-law corrections. Also, at symbol level $\rho \rightarrow 1$ and $\Gamma_{\text{cusp}} \rightarrow 4g^2$. Hence we require

$$\mathcal{E} \rightarrow \exp\left[g^2 \mathcal{E}^{(1)}\right] + \mathcal{O}(\hat{u}^1, \hat{v}^1, \hat{w}^1), \quad (4.1)$$

as $(\hat{u}, \hat{v}, \hat{w}) \rightarrow (0, 0, 0)$. This condition fixes 2 of the 3 parameters, but one linear combination vanishes (up to powers) at the origin, and so it cannot be fixed there.

At this point, we reconstructed the one-parameter symbol-level solution for the 58,128 coefficients of the weight 11 basis functions in terms of rational numbers. The rational reconstruction is not too difficult because, for the coefficient of the one-parameter ambiguity, the denominator is 2^{26} (or a factor thereof) for all but 766 of the 58,128 rational numbers. For the coefficient of the inhomogeneous part, the denominator is $3^2 \times 2^{26}$ (or a factor thereof) for all but 851 of the 58,128 rational numbers. Furthermore, the rational numbers with “bad” denominators are all associated with just 33 of the 1503 weight 11 parity-even basis functions. We know in advance which 33 basis functions they are, by inspecting previous seven-loop results expressed in the same basis. So we can multiply through by $3^2 \times 2^{26}$, require the coefficients to be integers, and reconstruct the rational coefficients for the 1470 other parity-even basis functions, and all 382 parity-odd basis functions. The remaining coefficients are few enough in number that we could solve for them directly over the rational numbers, since we generated all the equations over the rational numbers.

5 The full function

With the symbol fixed up to one parameter, we proceed to fix all the zeta-valued constants multiplying lower-weight functions, i.e. the “beyond-the-symbol” terms. In the first stage, we do so at the level of the weight 11 quintuple final entries.

5.1 At quintuple level

There are 215 parity-even and 36 parity-odd beyond-the-symbol functions in \mathcal{H}^{hex} at weight 11. Since there are 211 parity-even and 213 parity-odd quintuples, there are $211 \times 215 + 213 \times 36 = 53,033$ parameters to determine. This can be done in one stage, but it again requires using prime fields. The workhorse for constraining these parameters is again the pair relations in the 6th-5th slots from the back. We also impose dihedral symmetry. The solution to the pair and dihedral constraints has 65 parameters. Next we impose the vanishing of the remainder function \mathcal{R} in the strict collinear limits, which leaves 17 parameters.

At this point, we return to the origin. The value of the eight-loop remainder function at the origin is [56]

$$\mathcal{R}^{(8)} = c_1^{(8)} \sum_{i=1}^3 (\ln^2 \hat{u}_i + \ln \hat{u}_i \ln \hat{u}_{i+1}) + c_2^{(8)} \sum_{i=1}^3 \ln \hat{u}_i \ln \hat{u}_{i+1} + c_0^{(8)} + \mathcal{O}(\hat{u}, \hat{v}, \hat{w}), \quad (5.1)$$

where

$$\begin{aligned} c_1^{(8)} = & \frac{3622824549}{1280} \zeta_{14} - \frac{69069}{4} \zeta_8 (\zeta_3)^2 - 33948 \zeta_6 \zeta_3 \zeta_5 - 34650 \zeta_4 \zeta_3 \zeta_7 - 16974 \zeta_4 (\zeta_5)^2 \\ & - 28224 \zeta_2 \zeta_3 \zeta_9 - 26208 \zeta_2 \zeta_5 \zeta_7 - 156 \zeta_2 (\zeta_3)^4 \\ & - 55440 \zeta_3 \zeta_{11} - 49728 \zeta_5 \zeta_9 - 23820 (\zeta_7)^2 - 800 (\zeta_3)^3 \zeta_5, \end{aligned} \quad (5.2)$$

$$\begin{aligned} c_2^{(8)} = & \frac{3730480571}{640} \zeta_{14} + \frac{29821}{2} \zeta_8 (\zeta_3)^2 + 28344 \zeta_6 \zeta_3 \zeta_5 + 27300 \zeta_4 \zeta_3 \zeta_7 + 13356 \zeta_4 (\zeta_5)^2 \\ & + 18816 \zeta_2 \zeta_3 \zeta_9 + 17472 \zeta_2 \zeta_5 \zeta_7 + 120 \zeta_2 (\zeta_3)^4 + 320 (\zeta_3)^3 \zeta_5, \end{aligned} \quad (5.3)$$

$$\begin{aligned} c_0^{(8)} = & \frac{157718118308821}{3703808} \zeta_{16} - \frac{2180163}{16} \zeta_{10} (\zeta_3)^2 - 299677 \zeta_8 \zeta_3 \zeta_5 - \frac{688875}{2} \zeta_6 \zeta_3 \zeta_7 \\ & - \frac{337713}{2} \zeta_6 (\zeta_5)^2 - 441840 \zeta_4 \zeta_3 \zeta_9 - 406320 \zeta_4 \zeta_5 \zeta_7 - 2061 \zeta_4 (\zeta_3)^4 - 498960 \zeta_2 \zeta_3 \zeta_{11} \\ & - 447552 \zeta_2 \zeta_5 \zeta_9 - 214380 \zeta_2 (\zeta_7)^2 - 6240 \zeta_2 (\zeta_3)^3 \zeta_5 \\ & - 679536 \zeta_3 \zeta_{13} - 760320 \zeta_5 \zeta_{11} - 782640 \zeta_7 \zeta_9 - 8792 (\zeta_3)^2 (\zeta_5)^2 - 5880 (\zeta_3)^3 \zeta_7. \end{aligned} \quad (5.4)$$

We compute \mathcal{E} from this value for \mathcal{R} , and the lower-loop values given in ref. [26], using eq. (2.26). We then take its quintuple coproducts near the origin, and compare them with those of our 17-parameter ansatz. We find that all but 2 of the parameters are fixed. Note that the precise values of the eight-loop coefficients $c_i^{(8)}$ in eq. (5.1) do not matter yet, because we are still performing the analysis at weight 11, and the quintuple coproducts annihilate anything not containing at least a weight 5 function, which includes all of eq. (5.1). On the other hand, products of lower-loop terms from expanding the exponential in eq. (2.26) can contribute at weight 11, because they can result in more than four logarithms.

We fixed one of the two remaining beyond-the-symbol parameters by observing that in the symbol-level solution, there were not actually 424 linearly-independent quintuple final entries, but only 384, of which 199 are parity-even and 185 are parity-odd. We required there to be only the same 384 quintuple final entries at function level as well.

The final beyond-the-symbol parameter at the level of quintuples multiplies a function which is ζ_8 times a weight 8 function. The weight 8 function is dihedrally symmetric, vanishes in the strict collinear limit and at the origin — modulo terms with at least weight 4 in zeta values, which vanish at the level of quintuple coproducts. However, it is non-vanishing in the near-collinear limit, at the level of one flux-tube excitation. This limit can be accessed easily from the $(1, \hat{v}, \hat{v})$ line as $\hat{v} \rightarrow 0$, where the function has a nonvanishing $\hat{v}^1 \ln^4 \hat{v}$ behavior. Thus we use a single term in the flux-tube OPE prediction to fix the final quintuple-level parameter. We provide the final set of 384 linearly independent quintuple final entries in an ancillary file, `MHV8quintuples.txt`, along with a routine for constructing all the other quintuples via the various linear relations.

5.2 Constants beyond weight 11

There are additional constants of integration above weight 11, which we need to determine in order to completely specify the amplitude. We specify the constants at the point $(1, 1, 1)$, but we impose constraints determining them at the point $(1, 0, 0)$ — strict collinear vanishing of \mathcal{R} and the one flux-tube excitation OPE information — as well as consistency between the $(1, \hat{v}, \hat{v})$ and $(\hat{u}, 0, 0)$ lines where they intersect.

At weight 12, we have 166 linearly independent quadruple final entries to determine at the point $(1, 1, 1)$. However, the 82 parity-odd quadruples all vanish at $(1, 1, 1)$, since this point lies on the parity-preserving surface $\Delta = 0$. Also, using the branch-cut condition that $F^{1-\hat{u}} = 0$ for $\hat{u} \rightarrow 1$, for any function F , we know that

$$\mathcal{E}^{\hat{d},x,y,z}(1, 1, 1) = \mathcal{E}^{\hat{d},x,y,z}(1, 1, 1) = \mathcal{E}^{\hat{d},x,y,z}(1, 1, 1) = 0, \quad (5.5)$$

for any letters x, y, z . Combining this information with dihedral symmetry, we find only 10 independent weight 12 quadruple constants at $(1, 1, 1)$. Repeating the same exercise for the weight 13 triple constants yields only 3 independent ones. Similarly, there are 2 independent weight 14 double constants, no nonvanishing weight 15 single final entries, and one weight 16 constant value at $(1, 1, 1)$. Given these $10+3+2+0+1 = 16$ constants, we can integrate up the full function on the line $(1, \hat{v}, \hat{v})$, and then take $\hat{v} \rightarrow 0$ to access the soft endpoint of the strict collinear limit (at leading power in \hat{v} , namely \hat{v}^0) and a part of the one flux-tube excitation OPE information (at order \hat{v}^1). The result on the line $(1, \hat{v}, \hat{v})$ can be expressed in terms of HPLs [4] of the form $H_{\vec{a}}(\hat{v})$ with $a_i \in \{0, 1\}$. In carrying out this step, it is useful to be able to evaluate rather high-weight MZVs; we use the program `HYPERLOGPROCEDURES` [69] for this purpose. Of the 16 constants, only 10 actually appear in $\mathcal{E}^{(8)}(1, \hat{v}, \hat{v})$. Four of these are fixed by the strict collinear limit, and three more are fixed by the OPE information at order \hat{v}^1 .

Next we integrate up along the collinear limit line, not just the soft endpoint. The results are HPLs, $H_{\vec{a}}(\hat{u} = 1 - \hat{w})$ with $a_i \in \{0, 1\}$. However, we find only one more constraint, leaving 8 constants still to be fixed.

Finally, we construct the full function on the line $(\hat{u}, 0, 0)$. This means that \hat{u} has a generic value, while $\hat{v}, \hat{w} \ll 1$. The results are HPLs $H_{\vec{a}}(\hat{u})$, $a_i \in \{0, 1\}$, multiplied by polynomials in

$\ln \hat{v}$ and $\ln \hat{w}$. There are consistency conditions from matching the results on the $(1, \hat{v}, \hat{v})$ line, as $\hat{v} \rightarrow 0$, to the results on the $(\hat{u}, 0, 0)$ line, as $\hat{u} \rightarrow 1$. These consistency conditions suffice to fix all 8 of the undetermined constants. We then take the limit $\hat{u} \rightarrow 0$, to obtain the value of $\mathcal{E}^{(8)}$ at the origin. It agrees perfectly with the prediction (5.1).

We provide all the values of the weight 12, 13, 14, and 16 constants in the ancillary file `EZMHVcoproducts111.txt`, along with some lower-loop values (at weight 12 and above) and the ρ factor from eq. (2.29).

6 Checks

Besides checking the behavior at the origin, as just mentioned, we checked several other limits where the amplitude's behavior is well understood:

1. The self-crossing limit.
2. Multiparticle factorization limit.
3. Near-collinear (OPE) limit.
4. Multi-Regge kinematics (MRK).

In the remainder of this section we briefly describe these limits and checks.

6.1 Self-crossing limit

There is a limit of massless $2 \rightarrow 4$ scattering that mimics double parton scattering, in that the two incoming partons can each split into (almost on-shell) pairs of partons, and then two separate $2 \rightarrow 2$ scatterings take place. There is an analogous limit of $3 \rightarrow 3$ scattering, where one of the three incoming partons splits, and one of the three outgoing partons is a fusion of two almost on-shell outgoing partons. These kinematic limits have an interpretation in the dual Wilson hexagon as limits where two opposite sides of the hexagon almost cross each other [70]. (For earlier studies of the self-crossing limit, see refs. [71–73].) Logarithmic singularities are generated due to the exchange of virtual gluons between the two nearby sides. In ref. [26], an all-orders formula for the singular terms in this limit was presented, and it was checked against perturbative results through seven loops. Here we will check it at eight loops.

The singular terms have a simpler structure in the $3 \rightarrow 3$ case than in the $2 \rightarrow 4$ case because the hexagonal Wilson loop is quasi-Euclidean, with sides alternating between incoming and outgoing. In self-crossing kinematics, the cross ratios $(\hat{u}, \hat{v}, \hat{w})$ approach $(1 - \delta, \hat{v}, \hat{v})$ with $\delta \rightarrow 0$, after analytic continuation onto the correct sheet. Here δ is a dual-conformally-invariant measure of the separation of the two sides that are almost crossing. In the $3 \rightarrow 3$ case, the analytic continuation is $\hat{u} \rightarrow e^{+2\pi i} \hat{u}$, $\hat{v} \rightarrow e^{+\pi i} \hat{v}$, $\hat{w} \rightarrow e^{+\pi i} \hat{w}$. Also, $\delta \rightarrow 0$ from the negative side, and \hat{v} is either negative or greater than one [70]. All the

logarithmic singularities as $|\delta| \rightarrow 0$ appear in the imaginary part of the amplitude, and they are independent of \hat{v} . The all-orders formula is [26]:

$$\frac{1}{2\pi i} \frac{d\mathcal{E}_{3 \rightarrow 3}}{d \ln |\delta|} = \frac{g^2}{\rho} \exp\left[\frac{1}{2}\zeta_2 \Gamma_{\text{cusp}} + 2\Gamma_3\right] \times 2 \int_0^\infty d\nu J_1(2\nu) \exp\left[-\frac{\Gamma_{\text{cusp}}}{4} [\lambda(\nu)]^2 - \Gamma_{\text{virt}} \lambda(\nu)\right], \quad (6.1)$$

where J_1 is the first Bessel function and

$$\lambda(\nu) = 2(\ln \nu + \gamma_E) - \ln |\delta|, \quad (6.2)$$

with γ_E the Euler-Mascheroni constant. The anomalous dimensions Γ_3 and Γ_{virt} are given in ref. [26].

The perturbative expansions of eq. (6.1) were provided in ref. [26] through seven loops

(for the earlier value of ρ). Here we give the eight loop value, for ρ in eq. (2.29):

$$\begin{aligned}
\frac{1}{2\pi i} \frac{d\mathcal{E}_{3 \rightarrow 3}^{(8)}}{d \ln |\delta|} = & -\frac{1}{5040} \ln^{14} |\delta| - \frac{\zeta_2}{72} \ln^{12} |\delta| - \frac{17}{90} \zeta_3 \ln^{11} |\delta| - \frac{163}{120} \zeta_4 \ln^{10} |\delta| \\
& - \left(\frac{236}{15} \zeta_5 + \frac{77}{9} \zeta_2 \zeta_3 \right) \ln^9 |\delta| - \left(\frac{2963}{48} \zeta_6 + \frac{401}{9} (\zeta_3)^2 \right) \ln^8 |\delta| \\
& - \left(\frac{18142}{21} \zeta_7 + \frac{1384}{3} \zeta_2 \zeta_5 + \frac{1378}{3} \zeta_4 \zeta_3 \right) \ln^7 |\delta| \\
& - \left(\frac{130889}{72} \zeta_8 + \frac{56132}{15} \zeta_3 \zeta_5 + \frac{9452}{9} \zeta_2 (\zeta_3)^2 \right) \ln^6 |\delta| \\
& - \left(28504 \zeta_9 + 14860 \zeta_2 \zeta_7 + \frac{71672}{5} \zeta_4 \zeta_5 + \frac{28507}{3} \zeta_6 \zeta_3 + 2432 (\zeta_3)^3 \right) \ln^5 |\delta| \\
& - \left(\frac{2725139}{80} \zeta_{10} + \frac{260096}{3} \zeta_3 \zeta_7 + 42920 (\zeta_5)^2 + \frac{138584}{3} \zeta_2 \zeta_3 \zeta_5 \right. \\
& \quad \left. + \frac{71152}{3} \zeta_4 (\zeta_3)^2 \right) \ln^4 |\delta| \\
& - \left(446544 \zeta_{11} + 241696 \zeta_2 \zeta_9 + 218396 \zeta_4 \zeta_7 + 141348 \zeta_6 \zeta_5 + \frac{842009}{9} \zeta_8 \zeta_3 \right. \\
& \quad \left. + \frac{318304}{3} (\zeta_3)^2 \zeta_5 + \frac{64096}{3} \zeta_2 (\zeta_3)^3 \right) \ln^3 |\delta| \\
& - \left(\frac{3772896325}{11056} \zeta_{12} + 867552 \zeta_3 \zeta_9 + 827936 \zeta_5 \zeta_7 + 412160 \zeta_2 \zeta_3 \zeta_7 + 201696 \zeta_2 (\zeta_5)^2 \right. \\
& \quad \left. + 417272 \zeta_4 \zeta_3 \zeta_5 + 138546 \zeta_6 (\zeta_3)^2 + 18848 (\zeta_3)^4 \right) \ln^2 |\delta| \\
& - \left(1755072 \zeta_{13} + 1320480 \zeta_2 \zeta_{11} + 1048656 \zeta_4 \zeta_9 + 652370 \zeta_6 \zeta_7 + \frac{1258672}{3} \zeta_8 \zeta_5 \right. \\
& \quad \left. + \frac{3033977}{10} \zeta_{10} \zeta_3 + 459744 (\zeta_3)^2 \zeta_7 + 448960 \zeta_3 (\zeta_5)^2 + 285632 \zeta_2 (\zeta_3)^2 \zeta_5 \right. \\
& \quad \left. + 96800 \zeta_4 (\zeta_3)^3 \right) \ln |\delta| \\
& - \frac{622062547}{672} \zeta_{14} - 1827072 \zeta_3 \zeta_{11} - 1724160 \zeta_5 \zeta_9 - 835360 (\zeta_7)^2 - 565824 \zeta_2 \zeta_3 \zeta_9 \\
& - 519232 \zeta_2 \zeta_5 \zeta_7 - 633920 \zeta_4 \zeta_3 \zeta_7 - 309616 \zeta_4 (\zeta_5)^2 - 405020 \zeta_6 \zeta_3 \zeta_5 \\
& - \frac{398330}{3} \zeta_8 (\zeta_3)^2 - 115904 (\zeta_3)^3 \zeta_5 - 16000 \zeta_2 (\zeta_3)^4. \tag{6.3}
\end{aligned}$$

It matches perfectly the result found directly from the eight-loop amplitude.

6.2 Factorization limit

Amplitudes generically have universal factorizing behavior near multi-particle poles. Using integrability in planar $\mathcal{N} = 4$ SYM, an all-orders formula has been found for this factorization limit for the NMHV amplitude, which contains a pole at tree level. The limit takes two of the three cross-ratios large, and the other one “small”, but in practice it can be taken to be of order 1. The simplest way to take this limit is via the line $(\hat{u}, 1, \hat{u})$ by taking $\hat{u} \rightarrow \infty$. This NMHV limit was checked through 4 loops in ref. [24], and it holds to 7 loops as well [28].

It was also realized [74] that the MHV amplitude has a similar factorization behavior, even though it does not have a tree-level pole; instead one should take a kind of discontinuity of the limiting behavior. More precisely, it was found that the MHV and NMHV behavior is related by

$$D^{(L)}(z) \equiv \frac{z}{2} \frac{d^2 \mathcal{E}^{(L)}(1, 1/z, 1/z)}{dz^2} \Big|_{z \rightarrow 0} = E^{(L-1)}(1/z, 1, 1/z) \Big|_{z \rightarrow 0} + \mathcal{O}(z), \quad (6.4)$$

where $E^{(L-1)}(\hat{u}, \hat{v}, \hat{w})$ is the parity-even component of the NMHV amplitude at one-loop order lower, and we keep only the leading power terms in the equation as $z \rightarrow 0$. Due to the final entry condition, there are no logarithmic terms at leading power in $\mathcal{E}^{(L)}(1, 1/z, 1/z)$ as $z \rightarrow 0$. There is a constant, but it is removed by the derivatives in eq. (6.4). The contributions to eq. (6.4) come from terms of the form $z \ln^k z$ in $\mathcal{E}^{(L)}(1, 1/z, 1/z)$ with $k > 0$ only, hence the relation to a discontinuity. Note that the same definition of ρ should be used for $\mathcal{E}^{(L)}$ and $E^{(L-1)}$ in eq. (6.4).

Here we give the values of $D^{(L)}(z)$ computed from the MHV amplitude through eight loops:

$$D^{(1)}(z) = 1, \quad (6.5)$$

$$D^{(2)}(z) = -2L^2 - 2\zeta_2, \quad (6.6)$$

$$D^{(3)}(z) = 2L^4 + 16\zeta_2 L^2 + 4\zeta_3 L + \frac{83}{2}\zeta_4, \quad (6.7)$$

$$D^{(4)}(z) = -\frac{4}{3}L^6 - 28\zeta_2 L^4 - \frac{88}{3}\zeta_3 L^3 - 443\zeta_4 L^2 - (112\zeta_5 + 136\zeta_2 \zeta_3)L - \frac{3177}{4}\zeta_6 - 32(\zeta_3)^2, \quad (6.8)$$

$$D^{(5)}(z) = \frac{2}{3}L^8 + \frac{80}{3}\zeta_2 L^6 + \frac{152}{3}\zeta_3 L^5 + 1047\zeta_4 L^4 + \left(736\zeta_5 + \frac{2240}{3}\zeta_2 \zeta_3\right)L^3 + (11048\zeta_6 + 408(\zeta_3)^2)L^2 + (3140\zeta_7 + 3280\zeta_2 \zeta_5 + 5934\zeta_4 \zeta_3)L + \frac{916603}{48}\zeta_8 + 1316\zeta_3 \zeta_5 + 596\zeta_2 (\zeta_3)^2, \quad (6.9)$$

$$D^{(6)}(z) = -\frac{4}{15}L^{10} - \frac{52}{3}\zeta_2 L^8 - 48\zeta_3 L^7 - \frac{3790}{3}\zeta_4 L^6 - \left(\frac{7264}{5}\zeta_5 + \frac{4432}{3}\zeta_2 \zeta_3\right)L^5 - \left(\frac{65819}{2}\zeta_6 + \frac{4048}{3}(\zeta_3)^2\right)L^4 - \left(21640\zeta_7 + 21216\zeta_2 \zeta_5 + \frac{115924}{3}\zeta_4 \zeta_3\right)L^3 - \left(\frac{8062091}{24}\zeta_8 + 23112\zeta_3 \zeta_5 + 11928\zeta_2 (\zeta_3)^2\right)L^2 - (100464\zeta_9 + 95080\zeta_2 \zeta_7 + 166328\zeta_4 \zeta_5 + 201269\zeta_6 \zeta_3 + 2912(\zeta_3)^3)L - \frac{94215313}{160}\zeta_{10} - 35792\zeta_3 \zeta_7 - 17376(\zeta_5)^2 - 33800\zeta_2 \zeta_3 \zeta_5 - 31268\zeta_4 (\zeta_3)^2 \quad (6.10)$$

$$\begin{aligned}
D^{(7)}(z) = & \frac{4}{45}L^{12} + \frac{128}{15}\zeta_2L^{10} + \frac{280}{9}\zeta_3L^9 + \frac{2987}{3}\zeta_4L^8 + \left(\frac{23744}{15}\zeta_5 + \frac{4928}{3}\zeta_2\zeta_3\right)L^7 \\
& + \left(\frac{144206}{3}\zeta_6 + \frac{19376}{9}(\zeta_3)^2\right)L^6 + \left(49288\zeta_7 + \frac{242848}{5}\zeta_2\zeta_5 + \frac{269060}{3}\zeta_4\zeta_3\right)L^5 \\
& + \left(\frac{9748865}{8}\zeta_8 + \frac{270040}{3}\zeta_3\zeta_5 + \frac{142840}{3}\zeta_2(\zeta_3)^2\right)L^4 \\
& + \left(774368\zeta_9 + 719360\zeta_2\zeta_7 + 1261072\zeta_4\zeta_5 + \frac{4638080}{3}\zeta_6\zeta_3 + \frac{72224}{3}(\zeta_3)^3\right)L^3 \\
& + \left(\frac{50905899}{4}\zeta_{10} + 798224\zeta_3\zeta_7 + 380576(\zeta_5)^2 + 793472\zeta_2\zeta_3\zeta_5 + 744132\zeta_4(\zeta_3)^2\right)L^2 \\
& + \left(3793104\zeta_{11} + 3393600\zeta_2\zeta_9 + 5602166\zeta_4\zeta_7 + 6522082\zeta_6\zeta_5 + \frac{31319745}{4}\zeta_8\zeta_3\right. \\
& \quad \left.+ 297552(\zeta_3)^2\zeta_5 + 107088\zeta_2(\zeta_3)^3\right)L \\
& + \frac{2017876455195}{88448}\zeta_{12} + 1269296\zeta_3\zeta_9 + 1144752\zeta_5\zeta_7 + 1170064\zeta_2\zeta_3\zeta_7 \\
& + 556304\zeta_2(\zeta_5)^2 + 2064582\zeta_4\zeta_3\zeta_5 + \frac{2565617}{2}\zeta_6(\zeta_3)^2 + 10352(\zeta_3)^4, \tag{6.11}
\end{aligned}$$

$$\begin{aligned}
D^{(8)}(z) = & -\frac{8}{315}L^{14} - \frac{152}{45}\zeta_2L^{12} - \frac{688}{45}\zeta_3L^{11} - \frac{2882}{5}\zeta_4L^{10} - \left(\frac{17504}{15}\zeta_5 + \frac{11120}{9}\zeta_2\zeta_3\right)L^9 \\
& - \left(\frac{89039}{2}\zeta_6 + \frac{19168}{9}(\zeta_3)^2\right)L^8 - \left(\frac{1298288}{21}\zeta_7 + \frac{923072}{15}\zeta_2\zeta_5 + 115208\zeta_4\zeta_3\right)L^7 \\
& - \left(\frac{25200161}{12}\zeta_8 + \frac{818416}{5}\zeta_3\zeta_5 + \frac{791824}{9}\zeta_2(\zeta_3)^2\right)L^6 \\
& - \left(2035936\zeta_9 + 1899824\zeta_2\zeta_7 + \frac{16717616}{5}\zeta_4\zeta_5 + 4152190\zeta_6\zeta_3 + 68096(\zeta_3)^3\right)L^5 \\
& - \left(\frac{4378007151}{80}\zeta_{10} + \frac{10796672}{3}\zeta_3\zeta_7 + 1697152(\zeta_5)^2 + \frac{10838224}{3}\zeta_2\zeta_3\zeta_5\right. \\
& \quad \left.+ 3423104\zeta_4(\zeta_3)^2\right)L^4 \\
& - \left(33391008\zeta_{11} + 29783488\zeta_2\zeta_9 + 49137612\zeta_4\zeta_7 + 57381324\zeta_6\zeta_5\right. \\
& \quad \left.+ \frac{419455771}{6}\zeta_8\zeta_3 + \frac{8332640}{3}(\zeta_3)^2\zeta_5 + \frac{3025184}{3}\zeta_2(\zeta_3)^3\right)L^3 \\
& - \left(\frac{25976759893203}{44224}\zeta_{12} + 33830944\zeta_3\zeta_9 + 29944736\zeta_5\zeta_7 + 31742912\zeta_2\zeta_3\zeta_7\right. \\
& \quad \left.+ 14939104\zeta_2(\zeta_5)^2 + 56171500\zeta_4\zeta_3\zeta_5 + 35249431\zeta_6(\zeta_3)^2 + 295392(\zeta_3)^4\right)L^2 \\
& - \left(169405632\zeta_{13} + 146577312\zeta_2\zeta_{11} + 231088872\zeta_4\zeta_9 + 253004589\zeta_6\zeta_7\right. \\
& \quad \left.+ 289917579\zeta_8\zeta_5 + \frac{14566638681}{40}\zeta_{10}\zeta_3 + 12164928(\zeta_3)^2\zeta_7 + 11391680\zeta_3(\zeta_5)^2\right. \\
& \quad \left.+ 12311648\zeta_2(\zeta_3)^2\zeta_5 + 7857888\zeta_4(\zeta_3)^3\right)L \\
& - \frac{1374127004947}{1280}\zeta_{14} - 55664064\zeta_3\zeta_{11} - 47148096\zeta_5\zeta_9 - 22132160(\zeta_7)^2 \\
& - 49702240\zeta_2\zeta_3\zeta_9 - 43868896\zeta_2\zeta_5\zeta_7 - 82235944\zeta_4\zeta_3\zeta_7 - 38672640\zeta_4(\zeta_5)^2 \\
& - 96406097\zeta_6\zeta_3\zeta_5 - \frac{177982387}{3}\zeta_8(\zeta_3)^2 - 1596160(\zeta_3)^3\zeta_5 - 438880\zeta_2(\zeta_3)^4, \quad (6.12)
\end{aligned}$$

where $L = \ln z$.

These results agree with the limit (6.4) of the NMHV amplitude through six loops as given in ref. [26], after taking into account the different choice of ρ via eq. (2.30). The eight-loop MHV result agrees with the seven-loop NMHV result found in ref. [28]. Notice the strict sign alternation for all terms in $D^{(L)}(z)$ through eight loops, and also in eq. (6.3).

6.3 Near-collinear (OPE) limit

Another powerful check of the eight-loop MHV amplitude is provided by its behavior in the near-collinear limit in the Euclidean region. This behavior is governed, to any order in the coupling, by the Wilson loop (or Pentagon) Operator Product Expansion [35–38, 75–83]. The limit is usually described by the variables $T = e^{-\tau}$, $S = e^\sigma$, and $F = e^{i\phi}$, where $\hat{v} = T^2/(1 + T^2)$, and it is similar to the collinear limit $\hat{v} \rightarrow 0$, $\hat{u} + \hat{w} \rightarrow 1$, but now keeping power-suppressed terms in T (or v). There is a straightforward recipe for computing the first

couple of terms in the T expansion, which was carried out through seven loops for MHV in ref. [26], so we will not repeat it here.

In the ancillary file `RLncy.txt`, we provide the T^1 terms in the near-collinear limit of $\mathcal{R}^{(L)}$ through eight loops. They have the form $\mathcal{R}^{(L)} \sim T(F + 1/F)f^{(L)}(S)$, where $S^2 = (1 - u)/u \equiv y$. We write $f(S)$ in terms of iterated integrals $\text{Iy}(\vec{w}) \equiv G_{\vec{w}}(y)$. The file is large because there are tens of thousands of such iterated integrals in the eight loop expression. The OPE recipe at order T^1 involves a sum over residues in the rapidity of the single flux-tube excitation, which can be difficult to resum exactly. Instead we can expand the expressions in `RLncy.txt` around $S = 0$, which corresponds to truncating the residue sum. We provide the (much shorter) series expansions through S^{41} and through eight loops in the ancillary file `RLncyser.txt`.

They agree perfectly with all the OPE predictions we have computed. At eight loops, we evaluated the full residue sum out to S^{11} , and the $\ln^k T$ terms with $k \geq 4$ out to S^{41} .

6.4 Multi-Regge kinematics

The limit of high-energy $2 \rightarrow 4$ scattering with large rapidity separation between the four outgoing partons is referred to as multi-Regge kinematics (MRK). There is an analogous limit of $3 \rightarrow 3$ scattering which is slightly simpler (as in the self-crossing case). In this limit the Fourier-Mellin transform of the amplitude factorizes [84–86]. The all-orders behavior of the BFKL eigenvalue and impact factor that enter the factorization formula is now understood to all orders via integrability and analytic continuation from the near-collinear limit [58].

To take the MRK limit in $2 \rightarrow 4$ scattering kinematics, the cross ratio \hat{u} is first analytically continued out of the Euclidean region, $\hat{u} \rightarrow \hat{u}e^{-2\pi i}$, and then we send $\hat{u} \rightarrow 1$ while $\hat{v}, \hat{w} \rightarrow 0$, holding fixed the ratios

$$\frac{\hat{v}}{1 - \hat{u}} \equiv \frac{1}{|1 - z|^2}, \quad \frac{\hat{w}}{1 - \hat{u}} \equiv \frac{|z|^2}{|1 - z|^2}. \quad (6.13)$$

In this limit the parity-odd variables become

$$y_u = 1, \quad y_v = \frac{1 - \bar{z}}{1 - z}, \quad y_w = \frac{(1 - z)\bar{z}}{(1 - \bar{z})z}. \quad (6.14)$$

At each order in perturbation theory, large logarithms are developed in $(1 - \hat{u})$, or alternatively in $\tau \equiv \sqrt{\hat{v}\hat{w}} = (1 - \hat{u})|z|/|1 + z|^2$. The coefficients of each power of $\ln \tau$ are single-valued (real analytic) functions of $z \in \mathbb{C}$, in fact they are single-valued HPLs (SVHPLs) [87, 88] $\mathcal{L}_{\vec{a}}(z, \bar{z})$, $a_i \in \{0, 1\}$.

In particular, in the ancillary file `hexMRKL1-7.m` [59] to ref. [26] the limiting behavior of the MHV amplitudes and NMHV amplitudes were provided in terms of a certain Fourier-Mellin integral. Here we use the coupling normalization and other conventions in ref. [89], where the remainder function in the $3 \rightarrow 3$ MRK limit is given by,

$$\exp(\mathcal{R} - i\pi\delta_6)|_{\text{MRK}, 3 \rightarrow 3} = \cos\left(\pi \frac{\Gamma_{\text{cusp}}}{4} \ln |z|^2\right) - i\pi\Sigma(L_\tau), \quad (6.15)$$

where

$$\delta_6 = \frac{\pi\Gamma_{\text{cusp}}}{4} \ln\left(\frac{|z|^2}{|1-z|^4}\right), \quad (6.16)$$

and

$$L_\tau = \ln \tau, \quad \tau = \sqrt{\hat{v}\hat{w}}. \quad (6.17)$$

The Fourier-Mellin representation of Σ is

$$\Sigma(L_\tau) = \frac{g^2}{\pi} \sum_{m=-\infty}^{\infty} \left(\frac{z}{\bar{z}}\right)^{\frac{m}{2}} \mathcal{P} \int_{-\infty}^{\infty} \frac{d\nu |z|^{2i\nu}}{\nu^2 + \frac{n^2}{4}} \Phi_{\text{reg}}(\nu, m) e^{-L_\tau \omega(\nu, m)}, \quad (6.18)$$

where $\omega(\nu, m)$ is the BFKL eigenvalues, $\Phi_{\text{reg}}(\nu, m)$ is the impact factor, and \mathcal{P} stands for the principal part. The $2 \rightarrow 4$ MRK limit is expressed in terms of $\Sigma(L_\tau + i\pi)$:

$$\exp(\mathcal{R} + i\pi\delta_6)|_{\text{MRK}, 2 \rightarrow 4} = \cos\left(\pi \frac{\Gamma_{\text{cusp}}}{4} \ln |z|^2\right) + i\pi \Sigma(L_\tau + i\pi), \quad (6.19)$$

The perturbative expansion of Σ is

$$\Sigma(L_\tau) = \sum_{L=1}^{\infty} g^{2L} \sum_{n=0}^{L-1} \Sigma_n^{(L)} (L_\tau)^n. \quad (6.20)$$

In the ancillary file `MRKSigma.txt`, we provide the values of $\Sigma_n^{(L)}$ through $L = 8$ loops. Note that $\Sigma_n^{(8)}$ is a weight $15 - n$ SVHPL, because the amplitude has weight 16, of which weight 1 goes to the $2\pi i$ from analytic continuation, and n to $(L_\tau)^n$.

The values through seven loops are taken from ref. [26], re-expressed in terms of $\Sigma_n^{(L)}$. To get the eight-loop values, we used tables giving the $2 \rightarrow 4$ MRK behavior of all elements of \mathcal{H}^{hex} at weight 11, in order to specify the behavior of all the MHV quintuples in that limit. Then we integrated up the results from the quintuples to get $\mathcal{E}^{(8)}|_{\text{MRK}, 2 \rightarrow 4}$. The integration is straightforward using the definitions of the SVHPLs and the relations between coproducts on the MRK surface (holding $(1 - \hat{u})$ fixed) and those in the bulk:

$$F^z = F^w - F^{yw}, \quad F^{1-z} = -F^v - F^w - F^{yv} + F^{yw}. \quad (6.21)$$

However, the integration also requires specifying boundary conditions in the MRK limit at each weight from 12 to 16.

We transported the boundary conditions from the base point $(\hat{u}, \hat{v}, \hat{w}) = (1, 1, 1)$ along two different routes. One route was to construct the answer on the line $(\hat{u}, 1, 1)$, then take $\hat{u} \rightarrow \hat{u}e^{-2\pi i}$ to get on the $2 \rightarrow 4$ sheet, then return to the point $(1, 1, 1)$, or rather $(1 - \delta, 1, 1)$. Then we move down the $2 \rightarrow 4$ self-crossing line $(1 - \delta, \hat{v}, \hat{v})$ until $\hat{v} \rightarrow 0^+$, which approaches the limit of MRK in which $z \rightarrow 1, \bar{z} \rightarrow 1$. This route also gave us the higher weight constants for the self-crossing line. For the second route, we moved down the line $(1, \hat{v}, \hat{v})$ on the Euclidean sheet. Then we moved along the line $(\hat{u}, 0, 0)$ (i.e. where \hat{v}, \hat{w} are infinitesimal) to the origin. Next we took $\hat{u} \rightarrow \hat{u}e^{-2\pi i}$ to get on the $2 \rightarrow 4$ sheet, and then returned to the

MRK point $(1, 0, 0)$ along the line $(\hat{u}, 0, 0)$. In this case we approach the limit of MRK from a different direction, $z \rightarrow 0, \bar{z} \rightarrow \infty$. We used the program HYPERLOGPROCEDURES [69] to extract the $z \rightarrow 0, \bar{z} \rightarrow \infty$ limits of the SVHPLs. This route also gave us the higher weight constants at the origin, as a byproduct.

We got the same result via both routes, which is a useful cross-check of the integration procedure. Then we converted the result from \mathcal{E} to \mathcal{R} using eq. (2.26) and extracted the perturbative coefficients of $\Sigma(L_\tau + i\pi)$. We computed $\Sigma_n^{(8)}$ via the Fourier-Mellin integral for $n = 4, 5, 6, 7$, and the results agreed perfectly with the results obtained from the amplitude.

7 Multiple final entry relations

In this section we describe relations between the k^{th} final entries of the MHV and NMHV amplitudes that are independent of the loop order L . Such relations are very useful for bootstrapping in the coproduct formalism, because they can greatly reduce the number of initial parameters in an ansatz. With the help of parity decompositions, we will find that many of the relations have saturated or stabilized by seven loops, and we can use this information to find “bonus” final entry relations. We use the old alphabet $\mathcal{L}_{\text{hex}}^u$ to describe the relations because they seem to be somewhat simpler in that alphabet.

A useful table for understanding the saturation of the final entries with loop order is Table 1. This table gives the number of independent $\{n, 1, 1, \dots, 1\}$ coproducts of the MHV amplitudes. The numbers through $L = 7$ are from ref. [28]. The eight loop numbers only became available after the eight-loop computation was completed, of course. A green color is used when the $(L + 1, n)$ entry is the same as the (L, n) entry; it indicates saturation of the hexagon function space \mathcal{H}^{hex} at weight n . The numbers at weights $n = 6, 7$ and $L = 5, 6, 7$ are slightly smaller than the numbers in the corresponding Table 8 of ref. [31] because of the new all-orders cosmic normalization ρ . The smaller numbers indicate that ρ is a more optimal normalization than the previous ρ_{old} . A blue color is used when the $(L + 1, n + 2)$ entry is the same as the (L, n) entry; it indicates saturation of the space of k^{th} -final entries, where $k = 2L - n$.

7.1 MHV single final entries

The number of linearly independent k^{th} final entries generally stabilizes at a sufficiently high number of loops, for small enough k . For example, in Table 1 we see that there are 6 final entries ($k = 1$, or weight $n = 2L - 1$) for the MHV amplitude, not 9. This is not surprising, because the \bar{Q} equation [90, 91] leads to the three final-entry relations,

$$\mathcal{E}^{1-\hat{u}_i} = -\mathcal{E}^{\hat{u}_i}, \quad \text{or} \quad \mathcal{E}^{\hat{a}} = \mathcal{E}^{\hat{b}} = \mathcal{E}^{\hat{c}} = 0. \quad (7.1)$$

7.2 MHV double final entries

Table 1 also indicates that there are 21 MHV double final entries ($k = 2$, or weight $n = 2L - 2$). Inspecting them more closely, 12 are parity-even and 9 are parity-odd. How many MHV

weight n	0	1	2	3	4	5	6	7	8	9	10	11	12	13	14	15	16
$L = 1$	1	3	1														
$L = 2$	1	3	6	4	1												
$L = 3$	1	3	6	13	14	6	1										
$L = 4$	1	3	6	13	27	35	20	6	1								
$L = 5$	1	3	6	13	27	54	77	51	21	6	1						
$L = 6$	1	3	6	13	27	54	102	163	126	58	21	6	1				
$L = 7$	1	3	6	13	27	54	102	190	318	293	159	62	21	6	1		
$L = 8$	1	3	6	13	27	54	102	190	343	579	630	384	162	62	21	6	1

Table 1: The number of independent $\{n, 1, 1, \dots, 1\}$ coproducts of the MHV amplitudes $\mathcal{E}^{(L)}$ through $L = 8$ loops, at function level. The green and blue entries indicate, respectively, saturation of \mathcal{H}^{hex} at weight n and of the $(2L - n)^{\text{th}}$ -final entries, as explained in the text.

double final entries should we expect? In refs. [30, 31] it was remarked that for the hexagon function space as a whole, imposing the branch-cut conditions and the extended Steinmann relations iteratively leads to 40 independent pairs of adjacent symbol entries; that is, there are 41 adjacency relations among the $9 \times 9 = 81$ possible pairs of 9 letters. (Integrability alone provides only 26 relations.) Now let us also impose the MHV final-entry conditions (7.1), which are really $9 \times 3 = 27$ conditions, $\mathcal{E}^{x, 1-\hat{u}_i} = -\mathcal{E}^{x, \hat{u}_i}$ for any of the 9 letters x . The 40 adjacency relations and the 27 MHV final-entry conditions together constitute 56 independent relations, and they reduce the expected number of pairs to 25, 15 parity-even and 10 parity-odd.

The \bar{Q} equations also can be used to constrain the MHV double final entries [74]. There are six such relations, three even and three odd. We give them in the old alphabet $\mathcal{L}_{\text{hex}}^u$:

$$\mathcal{E}^{y_v, y_u} = \mathcal{E}^{y_w, y_u} - \mathcal{E}^{y_v, y_w} + \mathcal{E}^{y_v, y_v} + \mathcal{E}^{\hat{w}, \hat{u}}, \quad (7.2)$$

$$\mathcal{E}^{y_w, y_v} = \mathcal{E}^{y_u, y_v} - \mathcal{E}^{y_w, y_u} + \mathcal{E}^{y_w, y_w} + \mathcal{E}^{\hat{u}, \hat{v}}, \quad (7.3)$$

$$\mathcal{E}^{y_u, y_w} = \mathcal{E}^{y_v, y_w} - \mathcal{E}^{y_u, y_v} + \mathcal{E}^{y_u, y_u} + \mathcal{E}^{\hat{v}, \hat{w}}, \quad (7.4)$$

$$\mathcal{E}^{1-\hat{u}, y_u} = \mathcal{E}^{y_v, \hat{v}} - \mathcal{E}^{y_w, \hat{u}} - \mathcal{E}^{\hat{v}, y_w}, \quad (7.5)$$

$$\mathcal{E}^{1-\hat{v}, y_v} = \mathcal{E}^{y_w, \hat{w}} - \mathcal{E}^{y_u, \hat{v}} - \mathcal{E}^{\hat{w}, y_u}, \quad (7.6)$$

$$\mathcal{E}^{1-\hat{w}, y_w} = \mathcal{E}^{y_u, \hat{u}} - \mathcal{E}^{y_v, \hat{w}} - \mathcal{E}^{\hat{u}, y_v}. \quad (7.7)$$

However, these relations are automatically satisfied by the 25 independent pairs.

Since the number of independent functions in Table 1 has stabilized at 12 parity-even, and 9 parity-odd, there must be three parity-even and one parity-odd “bonus” relations. They

are found to be, in the old alphabet,

$$\mathcal{E}^{y_v, y_u} = \mathcal{E}^{y_u, y_v} + \mathcal{E}^{\hat{u}, \hat{u}} + \mathcal{E}^{1-\hat{u}, \hat{u}} - \mathcal{E}^{\hat{v}, \hat{v}} - \mathcal{E}^{1-\hat{v}, \hat{v}}, \quad (7.8)$$

$$\mathcal{E}^{y_w, y_v} = \mathcal{E}^{y_v, y_w} + \mathcal{E}^{\hat{v}, \hat{v}} + \mathcal{E}^{1-\hat{v}, \hat{v}} - \mathcal{E}^{\hat{w}, \hat{w}} - \mathcal{E}^{1-\hat{w}, \hat{w}}, \quad (7.9)$$

$$\mathcal{E}^{y_u, y_w} = \mathcal{E}^{y_w, y_u} + \mathcal{E}^{\hat{w}, \hat{w}} + \mathcal{E}^{1-\hat{w}, \hat{w}} - \mathcal{E}^{\hat{u}, \hat{u}} - \mathcal{E}^{1-\hat{u}, \hat{u}}, \quad (7.10)$$

$$\mathcal{E}^{1-\hat{u}, y_u} = -\mathcal{E}^{y_u, \hat{u}} - \mathcal{E}^{\hat{v}, y_w} + \mathcal{E}^{y_w, \hat{v}}. \quad (7.11)$$

The first three (even) equations permute into each other under cyclic permutations, and flips do not given anything new. The last (odd) equation (7.11) appears to be asymmetric, and dihedral permutations of it would naively seem to generate more equations, but they turn out to all be equivalent to this relation when taking into account the other 26 odd relations.

Using all these relations, we can take the 12 independent parity-even MHV double final entries to be

$$\{\mathcal{E}^{\hat{u}_i, \hat{u}_i}, \mathcal{E}^{1-\hat{u}_i, \hat{u}_i}, \mathcal{E}^{y_i, y_i}, \mathcal{E}^{y_i, y_{i+1}}\}, \quad i = 1, 2, 3. \quad (7.12)$$

The remaining 33 even double final entries are given by

$$\mathcal{E}^{y_v, y_u} = \mathcal{E}^{\hat{u}, \hat{u}} + \mathcal{E}^{1-\hat{u}, \hat{u}} - \mathcal{E}^{\hat{v}, \hat{v}} - \mathcal{E}^{1-\hat{v}, \hat{v}} + \mathcal{E}^{y_u, y_v}, \quad (7.13)$$

$$\mathcal{E}^{\hat{u}, \hat{v}} = \mathcal{E}^{\hat{v}, \hat{v}} + \mathcal{E}^{1-\hat{v}, \hat{v}} - \mathcal{E}^{\hat{w}, \hat{w}} - \mathcal{E}^{1-\hat{w}, \hat{w}} - \mathcal{E}^{y_w, y_w} - \mathcal{E}^{y_u, y_v} + \mathcal{E}^{y_v, y_w} + \mathcal{E}^{y_w, y_u}, \quad (7.14)$$

$$\mathcal{E}^{1-\hat{u}, \hat{v}} = \mathcal{E}^{\hat{u}, \hat{u}} + \mathcal{E}^{1-\hat{u}, \hat{u}} - \mathcal{E}^{\hat{v}, \hat{v}} - \mathcal{E}^{1-\hat{v}, \hat{v}} + \mathcal{E}^{y_w, y_w} + \mathcal{E}^{y_u, y_v} - \mathcal{E}^{y_v, y_w} - \mathcal{E}^{y_w, y_u}, \quad (7.15)$$

$$\mathcal{E}^{\hat{u}_i, 1-\hat{u}_j} = -\mathcal{E}^{\hat{u}_i, \hat{u}_j}, \quad (7.16)$$

$$\mathcal{E}^{1-\hat{u}_i, 1-\hat{u}_j} = -\mathcal{E}^{1-\hat{u}_i, \hat{u}_j}, \quad (7.17)$$

plus the dihedral images of these relations.

Similarly, we can take the 9 independent parity-odd MHV double final entries to be

$$\{\mathcal{E}^{\hat{u}_i, y_j}\}, \quad i, j = 1, 2, 3. \quad (7.18)$$

The remaining 27 odd double final entries follow from the relations,

$$\mathcal{E}^{1-\hat{u}, y_u} = \frac{1}{2} \left[\mathcal{E}^{\hat{v}, y_u} + \mathcal{E}^{\hat{w}, y_u} - \mathcal{E}^{\hat{u}, y_v} - \mathcal{E}^{\hat{w}, y_v} - \mathcal{E}^{\hat{u}, y_w} - \mathcal{E}^{\hat{v}, y_w} \right], \quad (7.19)$$

$$\mathcal{E}^{1-\hat{u}, y_v} = \mathcal{E}^{\hat{u}, y_u} + \mathcal{E}^{\hat{v}, y_u} + \mathcal{E}^{\hat{w}, y_u} - \mathcal{E}^{\hat{u}, y_v} - \mathcal{E}^{\hat{u}, y_w} - \mathcal{E}^{\hat{v}, y_w} - \mathcal{E}^{\hat{w}, y_w}, \quad (7.20)$$

$$\mathcal{E}^{y_u, \hat{u}} = \mathcal{E}^{\hat{u}, y_u}, \quad (7.21)$$

$$\mathcal{E}^{y_v, \hat{u}} = \frac{1}{2} \left[-\mathcal{E}^{\hat{v}, y_u} - \mathcal{E}^{\hat{w}, y_u} + \mathcal{E}^{\hat{u}, y_v} - \mathcal{E}^{\hat{w}, y_v} + \mathcal{E}^{\hat{u}, y_w} + \mathcal{E}^{\hat{v}, y_w} \right] + \mathcal{E}^{\hat{w}, y_w}, \quad (7.22)$$

$$\mathcal{E}^{y_i, 1-\hat{u}_j} = -\mathcal{E}^{y_i, \hat{u}_j}. \quad (7.23)$$

and their dihedral images.

7.3 MHV triple final entries

We can perform a similar analysis for the MHV triple final entries, $\mathcal{E}^{x, y, z}$, where x, y, z are generic letters. We require the last two slots (y, z) to be in the 21-dimensional space of MHV

weight n	0	1	2	3	4	5	6	7	8	9	10	11	12	13	14	15	16
$L \leq 7$	0	0	0	1	2	6	13	29	57	113	161	112	39	12	2	–	–
$L = 8$	0	0	0	1	2	6	13	29	57	113	193	185	78	31	9	3	0

Table 2: The number of parity odd $\{n, 1, 1, \dots, 1\}$ coproducts of the MHV and NMHV amplitudes through 7 loops, followed by the number for the 8 loop MHV amplitude alone. The color coding is the same as in Table 1.

double final entries, and the first two slots (x, y) to be in the generic 40-dimensional space of adjacent pairs. The first requirement gives $9 \times 60 = 540$ relations, and the second one $41 \times 9 = 369$ relations. Solving the equations, we find that there are 65 independent triple final entries, 34 parity-even and 31 parity-odd. Now we take the 58 and 62 triple final entries at six and seven loops, shown in Table 1, and determine their parity. There are 31 even and 27 odd at six loops, and 31 even and 31 odd at seven loops. Thus the even number has saturated, while the odd number already agrees with the analysis based on the double final entries and the general 40-pair restriction. Hence the number of MHV triple final entries shown in Table 1 has stabilized at 62, 31 even and 31 odd.

We also conclude that there must be three “bonus” triple final entry relations in the parity-even sector. By comparing the 34 parity-even functions inferred from the double-final-entry analysis with the actual 31 functions at six and seven loops, we find that the bonus relations can be written as,

$$\begin{aligned}
\mathcal{E}^{1-\hat{u},\hat{u},\hat{u}} &= \mathcal{E}^{\hat{u},1-\hat{u},\hat{u}} + 2\mathcal{E}^{y_u,\hat{u},y_u} + \mathcal{E}^{y_u,\hat{u},y_v} + \mathcal{E}^{y_u,\hat{u},y_w} + 5(\mathcal{E}^{y_u,\hat{v},y_u} + \mathcal{E}^{y_u,\hat{w},y_u}) \\
&\quad - 2(\mathcal{E}^{y_v,\hat{u},y_v} + \mathcal{E}^{y_w,\hat{u},y_w} - \mathcal{E}^{y_v,\hat{v},y_w} - \mathcal{E}^{y_w,\hat{w},y_v} + \mathcal{E}^{y_v,\hat{w},y_v} + \mathcal{E}^{y_w,\hat{v},y_w}) \\
&\quad - 4(\mathcal{E}^{y_v,\hat{v},y_u} + \mathcal{E}^{y_w,\hat{w},y_u}) + \mathcal{E}^{y_u,\hat{v},y_v} + \mathcal{E}^{y_u,\hat{w},y_w} - \mathcal{E}^{y_v,\hat{v},y_v} - \mathcal{E}^{y_w,\hat{w},y_w} \\
&\quad - \mathcal{E}^{y_w,\hat{v},y_v} - \mathcal{E}^{y_v,\hat{w},y_w} ,
\end{aligned} \tag{7.24}$$

plus the two equations obtained by cyclic permutations of this one. There is some arbitrariness in how the bonus relations are written, since they are modulo a large number of other relations. We have checked that eq. (7.24) holds for all loop orders through seven loops.

8 Parity decomposition of amplitude coproducts and locking

In Table 2 we provide the number of independent parity-odd $\{n, 1, 1, \dots, 1\}$ coproducts for the combined system of MHV and NMHV amplitudes through seven loops, followed by the number for the eight loop MHV amplitude alone. With the addition of this last amplitude, saturation of the odd functions is now achieved all the way through weight 9. These data allow us to see cleanly that the space of hexagon functions used in refs. [26, 31] can be reduced further in size.

weight n	0	1	2	3	4	5	6	7	8	9	10	11	12	13	14	15	16
$L \leq 7$	1	3	6	12	25	48	89	161	280	377	255	107	43	12	4	–	–
$L = 8$	1	3	6	12	25	48	89	161	286	466	437	199	84	31	12	3	1

Table 3: The number of parity even $\{n, 1, 1, \dots, 1\}$ coproducts of the MHV and NMHV amplitudes through 7 loops, followed by the number for the 8 loop MHV amplitude alone. The color coding is the same as in Table 1.

Starting at weight 7, the saturated number of parity-odd functions is lower than with the previous normalization factor ρ , due to the locking phenomenon mentioned in ref. [28]. At weight 7 odd, only one function is removed: $\zeta_4 \tilde{\Phi}_6$, where $\zeta_4 = \pi^4/90$ and $\tilde{\Phi}_6$ is the unique weight 3 parity-odd function, namely the $D = 6$ scalar hexagon integral.

This function must be added to the other 29, symbol-level weight 7 odd functions with fixed coefficients. In terms of the basis used in refs. [26, 31], which is called $\{\text{YO}[7, i]\}$, $i = 1, 2, \dots, 30$ in the ancillary files, the smaller 29-dimension space is

$$\{\text{YO}[7, i] + c_i^{7o} \text{YO}[7, 30]\}, \quad i = 1, 2, \dots, 29, \quad (8.1)$$

where $\text{YO}[7, 30] = \zeta_4 \tilde{\Phi}_6$, and

$$c_i^{7o} = [9, -12, -12, -12, -9, -9, 9, 48, -9, 3, -39, -18, -51, -6, 9, -30, 12, -21, 27, 15, 6, 3, -27, -6, 24, -30, 12, -33, -30]. \quad (8.2)$$

Notice that the coefficients are all a multiple of 3. This property holds also for all the analogous ζ_4 -associated coefficients for weight 8 and 9 odd and weight 6 and 7 even. The coefficients of $\text{YO}[9, 120] = \zeta_6 \tilde{\Phi}_6$ encountered at weight 9 odd are always integers, but not always a multiple of 3. The coefficients for all these linear combinations are provided in the ancillary file `EZsmallercoproductspace.txt`.

At weight 8 odd, two functions are removed, corresponding to ζ_4 times the two weight 4 odd functions. At weight 9 odd, seven functions are removed, corresponding to ζ_4 times the six weight 5 odd functions, plus ζ_6 times the one weight 3 odd function. In other words, the number of independent odd functions for weights 7,8,9 in the new normalization is exactly equal to the number of consistent symbols.

Table 3 provides the corresponding numbers in the parity-even sector. Comparing them with the numbers for the old amplitude normalization reveals the following: At weight 6 even, three functions are removed, corresponding to $\zeta_4 \text{Li}_2(1 - 1/u_i)$. However, the three pure logarithms $\zeta_4(\ln^2 a_i + 4\zeta_2)$ are still required to be independent functions. At weight 7 even, nine functions are removed, corresponding to ζ_4 multiplied by the weight 3 even functions containing $1 - u_i$ in their symbols, while the six functions $\zeta_4 \ln^3 a_i + \dots$ and $\zeta_6 \ln a_i$ are still independent functions. We don't have quite enough information yet to confirm this pattern past weight 7 in the parity-even sector. The number of weight 8 even functions obtained

through seven loops is 280, while for the eight loop MHV amplitude there are 286, so the number of functions may not have stabilized yet.

9 Amplitudes and multiple coproducts at $(1, 1, 1)$

In this section we examine the values of the amplitudes and their multiple coproducts at the dihedrally symmetric, finite base point, $(\hat{u}, \hat{v}, \hat{w}) = (1, 1, 1)$, where they evaluate to MZVs. They belong to a restricted set of MZVs, $\mathcal{H}^{\text{hex}}(1, 1, 1)$, which obeys a coaction principle [31]. The MHV 8-loop amplitude allows us to test the coaction principle further and search for “dropouts” that imply further constraints at higher weights. In addition, there are interesting relations between the multiple coproducts of the amplitudes at $(1, 1, 1)$, that hold at every loop order through $L = 8$, for which we do not yet have a complete explanation.

9.1 Coaction principle at $(1, 1, 1)$

Multiple polylogarithms have motivic versions which are subject to a coaction [60–62, 92, 93]. The coaction Δ (not to be confused with the polynomial Δ whose vanishing defines the parity-preserving surface!) maps a general space of polylogarithms \mathcal{G} essentially into two copies of itself,

$$\Delta(\mathcal{G}) = \mathcal{G} \otimes \mathcal{G}^{\text{dR}}. \quad (9.1)$$

The right “de Rham” space \mathcal{G}^{dR} loses some information about contours of integration and is therefore only defined modulo $i\pi$ (roughly; for a more detailed discussion see e.g. ref. [31]). Since \mathcal{G} is graded by the weight,

$$\mathcal{G} = \bigoplus_{n=0}^{\infty} \mathcal{G}_n, \quad (9.2)$$

Δ acting on \mathcal{G}_n can be split into components $\Delta_{n-p,p}$ according to the grading, where $p \in \mathbb{Z}$. The case $p = 1$ is the total differential, as discussed around eq. (2.19). Iterations of $\Delta_{n-1,1}$ lead to the symbol.

The coaction principle is a statement about the stability of the left-hand side of the coaction, for a subspace of a space of multiple polylogarithms (or perhaps MZVs, which are multiple polylogarithms evaluated at a particular point) that is picked out by a given physical problem. For the space of hexagon functions \mathcal{H}^{hex} , we ask whether it obeys

$$\Delta \mathcal{H}^{\text{hex}} \subset \mathcal{H}^{\text{hex}} \otimes \mathcal{K}^\pi. \quad (9.3)$$

Here \mathcal{K}^π involves iterated integrals whose symbols have the same pair-adjacency relations as in \mathcal{H}^{hex} , but they lack the first entry condition, so the space \mathcal{K}_n^π is much larger than $\mathcal{H}_n^{\text{hex}}$ for a given weight n .

Because we construct the space of hexagon functions \mathcal{H}^{hex} iteratively, by requiring their derivatives to be in the space, the part of the coaction principle that involves only $\Delta_{n-1,1}$ is automatically obeyed. The interesting question has to do with $\Delta_{n-p,p}$ for $p > 1$, and in particular with constants on the right-hand side of the coaction, since such constants are

invisible at the level of differentials ($\Delta_{n-1,1}$). Such constants can be seen by evaluating all the hexagon functions at the point $(1, 1, 1)$, and we refer to the space of MZVs there as $\mathcal{H}^{\text{hex}}(1, 1, 1)$. In ref. [31] it was found that only a restricted set of MZVs appears in $\mathcal{H}^{\text{hex}}(1, 1, 1)$, and that this set was stable under the coaction.

A way to represent MZVs which respects the coaction is to use an f -alphabet [61, 94]. In this description, each odd Riemann zeta value ζ_{2k+1} is mapped to a letter f_{2k+1} , for $k = 1, 2, 3, \dots$. If we take a free algebra $\mathbb{Q}(f_{2k+1})$ over the rational numbers, and supplement it with powers of π^2 , then that space is isomorphic to the vector space of the MZVs over the rationals. A free algebra means that the letters f_{2k+1} do not commute with each other; the different orderings allow for irreducible MZVs to be encoded. There is a derivation operation ∂_{2k+1} associated with every letter f_{2k+1} . It acts to remove any f_{2k+1} in the de Rham (right) factor of the coaction; if another $f_{2k'+1}$ is there it returns 0.

The antipode map associated with the coaction has a particularly simple action on MZVs in the f -alphabet: it simply reverses the ordering of all the f 's. Since it is only defined modulo the $i\pi$ ambiguity on the right-hand side of the coaction, one should ignore all π 's (and all even Riemann zeta values) in computing the antipode.

We use the f -alphabet version available in the program HYPERLOGPROCEDURES [69]. We write $f_{2k_1+1, 2k_2+1, \dots} \equiv f_{2k_1+1} f_{2k_2+1} \dots$ as a shorthand. We use an ordering convention of the f 's from refs. [69, 95] which is reversed with respect to our convention for the symbol; thus, the derivation ∂_{2k+1} acts on the *left* side of a string of f 's.

The following relations allow the conversion of the f -alphabet to more conventional MZV notation through weight 10:

$$f_{3,3} = \frac{1}{2}(\zeta_3)^2, \quad (9.4)$$

$$f_{5,3} = -\frac{1}{5}\zeta_{5,3}, \quad (9.5)$$

$$f_{3,3,3} = \frac{1}{6}(\zeta_3)^3, \quad (9.6)$$

$$f_{3,7} = \zeta_3\zeta_7 + \frac{1}{14}\left[3(\zeta_5)^2 + \zeta_{7,3}\right], \quad (9.7)$$

$$f_{7,3} = -\frac{1}{14}\left[3(\zeta_5)^2 + \zeta_{7,3}\right], \quad (9.8)$$

$$f_{5,5} = \frac{1}{2}(\zeta_5)^2. \quad (9.9)$$

The analogous conversions through weight 16 are given in the ancillary file `ftoMZV16.txt`. (See ref. [31] for conversions through weight 14.)

In the f alphabet, the vector space $\mathcal{H}^{\text{hex}}(1, 1, 1)$ was shown [31] to have the following

elements, through weight 12:

$$\begin{aligned}
& 1 \tag{9.10} \\
& - \\
& \zeta_2 \\
& - \\
& \zeta_4 \\
& 5f_5 - 2\zeta_2 f_3 \\
& \zeta_6 \\
& 7f_7 - \zeta_2 f_5 - 3\zeta_4 f_3 \\
& \zeta_8, \quad 5f_{3,5} - 2\zeta_2 f_{3,3} \\
& 7f_9 - 6\zeta_4 f_5, \quad 5f_9 - 3\zeta_6 f_3, \quad \zeta_2 f_7 - \zeta_6 f_3 \\
& \zeta_{10}, \quad 7f_{3,7} - \zeta_2 f_{3,5} - 3\zeta_4 f_{3,3}, \quad 5f_{5,5} - 2\zeta_2 f_{5,3} \\
& 33f_{11} - 20\zeta_8 f_3, \quad \zeta_2 f_9 - \zeta_8 f_3, \quad 3\zeta_4 f_7 - 2\zeta_8 f_3, \quad 3\zeta_6 f_5 - 2\zeta_8 f_3, \quad 5f_{3,3,5} - 2\zeta_2 f_{3,3,3} + \frac{5611}{132}\zeta_8 f_3 \\
& \zeta_{12}, \quad 7f_{3,9} - 6\zeta_4 f_{3,5}, \quad 5f_{3,9} - 3\zeta_6 f_{3,3}, \quad \zeta_2 f_{3,7} - \zeta_6 f_{3,3}, \quad 7f_{5,7} - \zeta_2 f_{5,5} - 3\zeta_4 f_{5,3}, \quad 5f_{7,5} - 2\zeta_2 f_{7,3}.
\end{aligned}$$

Notice that $\zeta_3 = f_3$ does not appear, and only one linear combination appears out of the two possible at weight 5, $5f_5 - 2\zeta_2 f_3$. These two facts, and the coaction principle, dictate that at weight 8, only ζ_8 and $5f_{3,5} - 2\zeta_2 f_{3,3}$ can appear. The first element, ζ_8 , like any even Riemann zeta value ζ_{2k} , gives nothing nontrivial (lower weight) under the coaction. For this reason, it is always allowed by the coaction principle. The second weight 8 MZV, $5f_{3,5} - 2\zeta_2 f_{3,3}$, is allowed because

1. ∂_5 annihilates it, acting on the left, which is necessary because $f_3 = \zeta_3$ is absent at weight 3 in eq. (9.10).
2. $\partial_3(5f_{3,5} - 2\zeta_2 f_{3,3}) = 5f_5 - 2\zeta_2 f_3$, which is proportional to the one linear combination in $\mathcal{H}_5^{\text{hex}}$.

Similarly, it is easy to see that the weight 10 basis is consistent with the coaction principle because, other than ζ_{10} , the basis elements are obtained by adding a “3” to the left of the one weight 7 basis element, and a “5” to the left of the one weight 5 basis element. In general one can add odd indices to the left of lower-weight basis elements, and also add either ζ_{2k} or f_{2k+1} to the basis, in order to get a candidate basis at the next weight that is consistent with the coaction principle.

We refer to the absence of f_3 , and of the other linear combination of f_5 and $\zeta_2 f_3$, as *dropouts*. These are missing zeta values whose absence is not required by the coaction principle. Without such dropouts, there would be no consequences of the coaction principle at (1, 1, 1). The number of dropouts at different weights in the list (9.10) is easily counted to be: 1 at weight 3, 1 at weight 5, 2 at weight 7, 1 at weight 9, 1 at weight 11.

It becomes increasingly difficult to establish the existence of dropouts at high weight, because as we will see later in this section, there can be relatively few independent amplitude coproducts at $(1, 1, 1)$. This is particularly true for odd weights, because the single coproducts for both MHV and NMHV amplitudes all vanish at $(1, 1, 1)$; and for MHV there are very few independent triple coproducts at $(1, 1, 1)$. However, with the benefit of all the eight-loop MHV amplitude coproducts, we can establish that all of the basis elements in the list (9.10) are present, with the exception of weight 12, where there is one dropout. Thus, the last line of eq. (9.10) should have only 5 entries instead of 6:

$$\begin{aligned}
& \left\{ \zeta_{12}, \quad 7f_{3,9} - 6\zeta_4 f_{3,5} + \frac{1}{3}(7f_{5,7} - \zeta_2 f_{5,5} - 3\zeta_4 f_{5,3}), \right. \\
& \quad 7(5f_{3,9} - 3\zeta_6 f_{3,3}) + \frac{5}{3}(7f_{5,7} - \zeta_2 f_{5,5} - 3\zeta_4 f_{5,3}), \quad \zeta_2 f_{3,7} - \zeta_6 f_{3,3}, \\
& \quad \left. 3(5f_{3,9} - 3\zeta_6 f_{3,3}) - (5f_{7,5} - 2\zeta_2 f_{7,3}) \right\} \tag{9.11} \\
= & \left\{ \zeta_{12}, \quad 7f_{3,9} + \frac{7}{3}f_{5,7} - \frac{1}{3}\zeta_2 f_{5,5} - \zeta_4(f_{5,3} + 6f_{3,5}), \right. \\
& \quad 35f_{3,9} + \frac{35}{3}f_{5,7} - \frac{5}{3}\zeta_2 f_{5,5} - 5\zeta_4 f_{5,3} - 21\zeta_6 f_{3,3}, \quad \zeta_2 f_{3,7} - \zeta_6 f_{3,3}, \\
& \quad \left. 15f_{3,9} - 5f_{7,5} + 2\zeta_2 f_{7,3} - 9\zeta_6 f_{3,3} \right\}. \tag{9.12}
\end{aligned}$$

The first form makes clear the linear combinations of the previous basis elements, and that it obeys the coaction principle. The 6-loop amplitudes $\mathcal{E}^{(6)}(1, 1, 1)$ and (NMHV) $E^{(6)}(1, 1, 1)$ are linear combinations of these 5 basis elements, as well as the 7-loop double coproducts of $\mathcal{E}^{(7)}$, $E^{(7)}$ and (NMHV parity-odd) $\tilde{E}^{(7)}$.

The independent quadruple coproducts of $\mathcal{E}^{(8)}$ at $(1, 1, 1)$ furnish a more stringent test of eq. (9.11). As mentioned in section 5.2, there are 10 such eight-loop constants before imposing more detailed constraints. The fact that they all live in the same 5-dimensional space provides convincing evidence of the first dropout to appear at an even weight.

At weight 13, the coaction principle allows for 9 possible basis elements. However, there is only one independent triple coproduct of $\mathcal{E}^{(8)}$ at $(1, 1, 1)$, and no single coproduct of $\mathcal{E}^{(7)}$, so we are unable to search for dropouts at weight 13 (or higher).

9.2 Amplitude at (1, 1, 1)

The value of the eight-loop MHV 6-point amplitude at $u = v = w = 1$ provides us with one weight 16 MZV. In terms of the f -alphabet, it is:

$$\begin{aligned}
\mathcal{E}^{(8)}(1, 1, 1) = & \mathbf{9122624} f_{9,7} + \mathbf{11543472} f_{7,9} + \mathbf{5153280} f_{11,5} + \mathbf{19603536} f_{5,11} + \mathbf{23915376} f_{3,13} \\
& + \mathbf{371520} f_{5,3,3,5} + \mathbf{400320} f_{3,3,5,5} + \mathbf{400320} f_{3,5,3,5} + \mathbf{825216} f_{3,3,3,7} \\
& - \zeta_2 (701856 f_{7,7} + 1303232 f_{9,5} + 430656 f_{5,9} + 2061312 f_{11,3} - 309696 f_{3,11} \\
& \quad + 160128 f_{3,5,3,3} + 160128 f_{3,3,5,3} + 117888 f_{3,3,3,5} + 148608 f_{5,3,3,3}) \\
& - \zeta_4 (3243888 f_{5,7} + 3475296 f_{7,5} + 3909696 f_{9,3} + 3215472 f_{3,9} + 353664 f_{3,3,3,3}) \\
& - \zeta_6 (3612804 f_{5,5} + 3791520 f_{7,3} + 3409152 f_{3,7}) - \zeta_8 (3720664 f_{5,3} + 3456614 f_{3,5}) \\
& - \frac{19560489}{5} \zeta_{10} f_{3,3} - \frac{512193667550809}{7639104} \zeta_{16}. \tag{9.13}
\end{aligned}$$

It is straightforward to check that application of ∂_{2k+1} to this results lands in the basis (9.10) for $k = 1, 2, 3, 4, 5, 6, 7$, as required by the coaction principle.

As mentioned above, to apply the antipode map to this expression, one only has to reverse the ordering of the f indices, and ignore any term with an $i\pi$ (none here) or a π^2 or an even Riemann zeta value ζ_{2k} . That means focusing on the integers shown in blue in eq. (9.13). Reversing the ordering of the f subscripts in these terms, we recover the appropriate value of the eight-loop form factor given in the ancillary file `AntipodePointsSummary.txt` for ref. [53] (modulo π^2 terms). Thus we confirm that antipodal duality works at eight loops beyond symbol level. Although antipodal duality was used in the construction of the amplitude, it was only used at symbol level, so this is quite a nice confirmation of its full action. We also confirmed antipodal duality at eight loops beyond symbol level on the entire line $(1, \hat{v}, \hat{v})$, using the prediction in the ancillary file `A6line1vv.dat` for ref. [53], and comparing it with the results in the ancillary file `EZMHVg_uu1_lin.txt`.

In terms of conventional MZVs, the eight-loop value at (1, 1, 1) is

$$\begin{aligned}
\mathcal{E}^{(8)}(1, 1, 1) = & \frac{4901904}{11} \zeta_{11,5} - 2764512 \zeta_{13,3} + 58944 \zeta_{7,3,3,3} - 54720 \zeta_{5,5,3,3} + 576 (\zeta_{5,3})^2 \\
& + 54720 \zeta_3 \zeta_{5,5,3} - 58944 \zeta_3 \zeta_{7,3,3} + 5760 \zeta_5 \zeta_{5,3,3} + 29472 (\zeta_3)^2 \zeta_{7,3} - \frac{57222368}{11} \zeta_7 \zeta_9 \\
& + 3016464 \zeta_5 \zeta_{11} + 23915376 \zeta_3 \zeta_{13} + 188496 (\zeta_3)^2 (\zeta_5)^2 + 137536 (\zeta_3)^3 \zeta_7 \\
& + \zeta_2 \left(1799904 \zeta_{11,3} - 411968 \zeta_{9,5} + 6144 \zeta_{5,3,3,3} - 8448 \zeta_3 \zeta_{5,3,3} + 4224 (\zeta_3)^2 \zeta_{5,3} \right. \\
& \quad \left. + 5485728 (\zeta_7)^2 + 7035328 \zeta_5 \zeta_9 - 4161408 \zeta_3 \zeta_{11} - 19648 (\zeta_3)^3 \zeta_5 \right) \\
& + \zeta_4 \left(259312 \zeta_{9,3} - 1910928 \zeta_5 \zeta_7 - 4448304 \zeta_3 \zeta_9 - 14736 (\zeta_3)^4 \right) \\
& + \zeta_6 \left(56784 \zeta_{7,3} - 1550370 (\zeta_5)^2 - 3217728 \zeta_3 \zeta_7 \right) + \zeta_8 \left(57930 \zeta_{5,3} - 3421414 \zeta_3 \zeta_5 \right) \\
& - \frac{19560489}{10} \zeta_{10} (\zeta_3)^2 - \frac{512193667550809}{7639104} \zeta_{16}. \tag{9.14}
\end{aligned}$$

We give this value (and its f -alphabet form) in the ancillary file `EZMHVcoproducts111.txt`. We give its numerical value in eq. (11.1) below.

9.3 Amplitude coproducts at $(1, 1, 1)$

Now we turn to relations among the MHV amplitude's multiple coproducts at $(1, 1, 1)$. In ref. [28], the subspace of MZVs encountered by evaluating the single, double and triple coproducts for both MHV and NMHV 6-particle amplitudes at $(1, 1, 1)$ is explored through 7 loops. The MHV structure is particularly simple, and we verify here that it continues to be obeyed through 8 loops. In this discussion, we use the old alphabet $\mathcal{L}_{\text{hex}}^u$ because the equations are a little shorter.

For MHV, the $\{2L - 1, 1\}$ first coproducts of the amplitudes must all vanish at $(1, 1, 1)$. This result follows from parity, the branch-cut condition that $\mathcal{E}^{1-\hat{u}_i}$ vanishes at $\hat{u}_i = 1$ [21, 31], and the final-entry condition $\mathcal{E}^{\hat{u}_i} = -\mathcal{E}^{1-\hat{u}_i}$.

In ref. [28] it is shown that all of the double coproducts of the MHV amplitudes at $(1, 1, 1)$ either vanish or can be expressed in terms of $\mathcal{E}^{\hat{u}, \hat{u}}(1, 1, 1)$ and $\mathcal{E}^{y_u, y_u}(1, 1, 1)$:

$$\mathcal{E}^{\hat{u}, 1-\hat{v}}(1, 1, 1) = \mathcal{E}^{\hat{u}, \hat{v}}(1, 1, 1) = \mathcal{E}^{1-\hat{u}, \hat{v}}(1, 1, 1) = \mathcal{E}^{1-\hat{u}, \hat{u}}(1, 1, 1) = 0, \quad (9.15)$$

$$\mathcal{E}^{\hat{u}, 1-\hat{u}}(1, 1, 1) = -\mathcal{E}^{\hat{u}, \hat{u}}(1, 1, 1), \quad (9.16)$$

$$\mathcal{E}^{y_u, y_v}(1, 1, 1) = \mathcal{E}^{y_u, y_u}(1, 1, 1), \quad (9.17)$$

including also the dihedral images of these relations, and the vanishing of parity-odd double coproducts. Hence to specify all MHV double coproducts at $(1, 1, 1)$ it is enough to tabulate $\mathcal{E}^{\hat{u}, \hat{u}}(1, 1, 1)$ and $\mathcal{E}^{y_u, y_u}(1, 1, 1)$ through 8 loops. The tabulation through 7 loops is provided in ref. [28]; here we give the 8 loop values:

$$\begin{aligned} \mathcal{E}^{(8)\hat{u}, \hat{u}}(1, 1, 1) &= -2246816 \left[f_{3,11} - \frac{20}{33} \zeta_8 f_{3,3} \right] + \frac{151360}{3} \left[\zeta_2 f_{3,9} - \zeta_8 f_{3,3} \right] \\ &+ 120224 \left[3\zeta_4 f_{3,7} - 2\zeta_8 f_{3,3} \right] + \frac{370232}{3} \left[3\zeta_6 f_{3,5} - 2\zeta_8 f_{3,3} \right] \\ &- 11264 \left[5f_{3,3,3,5} - 2\zeta_2 f_{3,3,3,3} + \frac{5611}{132} \zeta_8 f_{3,3} \right] - 65056 \left[7f_{5,9} - 6\zeta_4 f_{5,5} \right] \\ &- 146176 \left[5f_{5,9} - 3\zeta_6 f_{5,3} \right] + 73536 \left[\zeta_2 f_{5,7} - \zeta_6 f_{5,3} \right] \\ &- 130304 \left[7f_{7,7} - \zeta_2 f_{7,5} - 3\zeta_4 f_{7,3} \right] \\ &- \frac{331136}{3} \left[5f_{9,5} - 2\zeta_2 f_{9,3} \right] - \frac{42437345879}{30240} \zeta_{14} \end{aligned} \quad (9.18)$$

$$\begin{aligned} &= -197536\zeta_{9,5} + 693536\zeta_{11,3} - 11264\zeta_{5,3,3,3} + 11264\zeta_3\zeta_{5,3,3} - 5632(\zeta_3)^2\zeta_{5,3} \\ &+ 2976704(\zeta_7)^2 + \frac{8868512}{3}\zeta_5\zeta_9 - 2246816\zeta_3\zeta_{11} - \frac{28160}{3}(\zeta_3)^3\zeta_5 \\ &- \zeta_2 \left[\frac{394688}{9}\zeta_{9,3} + \frac{568768}{3}\zeta_5\zeta_7 - \frac{1672000}{3}\zeta_3\zeta_9 - \frac{2816}{3}(\zeta_3)^4 \right] \\ &- \zeta_4(2160\zeta_{7,3} - 188688(\zeta_5)^2 - 394464\zeta_3\zeta_7) - \zeta_6(4584\zeta_{5,3} - 342072\zeta_3\zeta_5) \\ &+ \frac{517768}{3}\zeta_8(\zeta_3)^2 - \frac{42437345879}{30240}\zeta_{14}, \end{aligned} \quad (9.19)$$

and

$$\begin{aligned}
\mathcal{E}^{(8) y_u, y_u}(1, 1, 1) &= 5593216 \left[f_{3,11} - \frac{20}{33} \zeta_8 f_{3,3} \right] - \frac{374816}{3} \left[\zeta_2 f_{3,9} - \zeta_8 f_{3,3} \right] \\
&\quad - 318400 \left[3\zeta_4 f_{3,7} - 2\zeta_8 f_{3,3} \right] - \frac{993784}{3} \left[3\zeta_6 f_{3,5} - 2\zeta_8 f_{3,3} \right] \\
&\quad + 24448 \left[5f_{3,3,3,5} - 2\zeta_2 f_{3,3,3,3} + \frac{5611}{132} \zeta_8 f_{3,3} \right] + 208292 \left[7f_{5,9} - 6\zeta_4 f_{5,5} \right] \\
&\quad + 484724 \left[5f_{5,9} - 3\zeta_6 f_{5,3} \right] - 235488 \left[\zeta_2 f_{5,7} - \zeta_6 f_{5,3} \right] \\
&\quad + 483712 \left[7f_{7,7} - \zeta_2 f_{7,5} - 3\zeta_4 f_{7,3} \right] \\
&\quad + \frac{1304416}{3} \left[5f_{9,5} - 2\zeta_2 f_{9,3} \right] - \frac{323971645187}{30240} \zeta_{14} \tag{9.20} \\
&= 430784\zeta_{9,5} - 1496656\zeta_{11,3} + 24448\zeta_{5,3,3,3} - 24448\zeta_3\zeta_{5,3,3} + 12224(\zeta_3)^2\zeta_{5,3} \\
&\quad - 5677624(\zeta_7)^2 - \frac{15172576}{3}\zeta_5\zeta_9 + 5593216\zeta_3\zeta_{11} + \frac{61120}{3}(\zeta_3)^3\zeta_5 \\
&\quad + \zeta_2 \left[\frac{981664}{9}\zeta_{9,3} + \frac{1256864}{3}\zeta_5\zeta_7 - \frac{3675296}{3}\zeta_3\zeta_9 - \frac{6112}{3}(\zeta_3)^4 \right] \\
&\quad + \zeta_4(35424\zeta_{7,3} - 518604(\zeta_5)^2 - 1028544\zeta_3\zeta_7) + \zeta_6(57204\zeta_{5,3} - 932664\zeta_3\zeta_5) \\
&\quad - \frac{1389512}{3}\zeta_8(\zeta_3)^2 - \frac{323971645187}{30240}\zeta_{14}. \tag{9.21}
\end{aligned}$$

The weight 14 values (9.18) and (9.20) also obey the coaction principle. In the ancillary file `EZMHVcoproducts111.txt` we give the double coproducts in the alphabet $\mathcal{L}_{\text{hex}}^a$.

Finally we discuss the values of the MHV triple coproducts at $(1, 1, 1)$. Empirically, they obey the following relations:

$$\begin{aligned}
\mathcal{E}^{\hat{u}, \hat{u}, \hat{u}}(1, 1, 1) &= \mathcal{E}^{\hat{v}, \hat{v}, \hat{u}}(1, 1, 1) = -\mathcal{E}^{\hat{v}, \hat{w}, \hat{u}}(1, 1, 1) = \mathcal{E}^{y_u, y_u, \hat{u}}(1, 1, 1) = \mathcal{E}^{y_u, y_v, \hat{u}}(1, 1, 1) \\
&= \mathcal{E}^{y_v, y_u, \hat{u}}(1, 1, 1) = \mathcal{E}^{y_v, y_v, \hat{u}}(1, 1, 1) = \mathcal{E}^{y_v, y_w, \hat{u}}(1, 1, 1) = \mathcal{E}^{y_u, \hat{u}, y_u}(1, 1, 1) \\
&= \mathcal{E}^{y_v, \hat{u}, y_u}(1, 1, 1) = \mathcal{E}^{\hat{u}, y_u, y_u}(1, 1, 1) = \mathcal{E}^{\hat{u}, y_v, y_u}(1, 1, 1), \tag{9.22}
\end{aligned}$$

where we omitted giving: values with $1 - \hat{u}$ in the final entry, which are of course related by $\mathcal{E}^{1-\hat{u}} = -\mathcal{E}^{\hat{u}}$; values related by the total dihedral symmetry of the MHV amplitude; and vanishing values. Thus, somewhat remarkably, all MHV triple coproducts are either 0 or $\pm \mathcal{E}^{\hat{u}, \hat{u}, \hat{u}}(1, 1, 1)$. The values of $\mathcal{E}^{\hat{u}, \hat{u}, \hat{u}}(1, 1, 1)$ through seven loops are given in ref. [28]. The

eight loop value is:

$$\begin{aligned}
\mathcal{E}^{(8)\hat{u},\hat{u},\hat{u}}(1,1,1) &= 6672 \left[5f_{3,5,5} - 2\zeta_2 f_{3,5,3} \right] + 6672 \left[5f_{5,3,5} - 2\zeta_2 f_{5,3,3} \right] \\
&+ 9824 \left[7f_{3,3,7} - \zeta_2 f_{3,3,5} - 3\zeta_4 f_{3,3,3} \right] + 1992948 f_{13} + 25808 \zeta_2 f_{11} \\
&- 267956 \zeta_4 f_9 - 284096 \zeta_6 f_7 - \frac{1728307}{6} \zeta_8 f_5 - \frac{6520163}{20} \zeta_{10} f_3 \quad (9.23) \\
&= 4560 \zeta_{5,5,3} - 4912 \zeta_{7,3,3} + 4912 \zeta_3 \zeta_{7,3} + 1992948 \zeta_{13} + 31416 \zeta_3 (\zeta_5)^2 \\
&+ 34384 (\zeta_3)^2 \zeta_7 - \zeta_2 (704 \zeta_{5,3,3} - 704 \zeta_3 \zeta_{5,3} + 346784 \zeta_{11} + 4912 (\zeta_3)^2 \zeta_5) \\
&- \zeta_4 (370692 \zeta_9 + 4912 (\zeta_3)^3) - 268144 \zeta_6 \zeta_7 - \frac{1710707}{6} \zeta_8 \zeta_5 \\
&- \frac{6520163}{20} \zeta_{10} \zeta_3. \quad (9.24)
\end{aligned}$$

The value $\mathcal{E}^{(8)\hat{a},\hat{a},\hat{d}}(1,1,1)$ in the alphabet $\mathcal{L}_{\text{hex}}^a$ is given in `EZMHVcoproducts111.txt`; they are related by $\mathcal{E}^{(8)\hat{u},\hat{u},\hat{u}}(1,1,1) = -2 \mathcal{E}^{(8)\hat{a},\hat{a},\hat{d}}(1,1,1)$

The values of the 166 (mostly) linearly independent weight 12 quadruple coproducts at $(1,1,1)$ are also provided in the ancillary file `EZMHVcoproducts111.txt`. We find that there are 5 independent values, which span the basis (9.11), indicating that there is a weight 12 dropout, as discussed in section 9.1.

10 Weight 16 Z functions

In the context of using antipodal duality to determine the MHV amplitude, it is of general interest to know how many independent parity-even hexagon functions vanish identically on the parity-preserving surface, and what other properties they might have. All the examples we have found so far, through weight 16, have the property that their parity-even first coproducts Z^{e_i} vanish identically, in the entire $(\hat{u}, \hat{v}, \hat{w})$ space. We call such functions Z functions. They are completely characterized by their odd first coproducts, Z^{y_i} . They only seem to appear at even weight. At weight 12, there is a single Z function, mentioned in ref. [26]. At weight 14, there is a triplet of such functions⁴, which permute into each other under cyclic symmetry, and whose cyclic sum is the function \tilde{Z} mentioned in ref. [26].

At weight 16 we found 9 such functions at symbol level. They form 3 separate triplets under the dihedral symmetry. (One linear combination of the 3 dihedrally-invariant symbols vanishes at the origin, at symbol level.) All the Z functions obey the same final entry conditions as the MHV amplitude \mathcal{E} , and addition relations that follow from setting $Z^{e_i} \rightarrow 0$, see Table 4 for the number of independent multi-final entries. We integrated up all of the weight 12, 14 and 16 Z functions from symbol-level to functions. We could do this uniquely, up to the existence of one beyond-the-symbol parameter at weight 16, which is none other than the weight 12 Z function multiplied by the zeta value ζ_4 , which has a free coefficient in

⁴We thank Ömer Gürdoğan for discussions on this subject.

function	singles	doubles	triples	quadruples	quintuples
\mathcal{E}	6	21	62	166	424
Z	3	6	14	31	70

Table 4: The number of independent multi-final entries for the MHV amplitude \mathcal{E} , compared with those for the Z functions. The latter are a subspace of the former.

\mathcal{H}^{hex} . (On the other hand, ζ_2 and ζ_3 do *not* have free coefficients, and the next free one is ζ_6 .)

10.1 Behavior at $(1, 0, 0)$

In ref. [31] it was mentioned that the space \mathcal{H}^{hex} constructed there was slightly over-complete, starting with the parity-even weight 8 functions, where 3 functions should be removed because they lead to irreducible MZVs, $\zeta_{5,3}$ in this case, at the points $(1, 0, 0)$, $(0, 1, 0)$ and $(0, 0, 1)$. If the space \mathcal{H}^{hex} is defined to be the minimal space containing all the coproducts of the MHV and NMHV amplitudes to all loop orders, then these 3 functions should not be in the space. That's because the OPE approach [36] implies that these limits can only contain Riemann zeta values, not irreducible MZVs such as $\zeta_{5,3}$. It is worth examining the multiple coproducts of the Z functions at $(1, 0, 0)$, etc., to see if any of these ambiguity functions can be discarded based on this function-level information.

In fact, we find that all the independent single, double, and triple coproducts of the Z functions at weights 12, 14 and 16 vanish completely at $(\hat{u}, \hat{v}, \hat{w}) = (1, 0, 0)$ (and at its cyclic images)! As shown in Table 4, there are 31 independent quadruple final entries, 15 parity-even and 16 parity-odd. The 16 odd quadruples have to vanish at $(1, 0, 0)$, but so do 14 of the 15 even ones. The 15 even quadruples can be taken to be

$$\begin{aligned}
& [\hat{d}, y_v, \hat{e}, y_v], [\hat{d}, y_v, \hat{f}, y_w], [\hat{f}, y_w, \hat{e}, y_v], [y_u, \hat{e}, \hat{f}, y_w], [y_v, \hat{e}, \hat{e}, y_v], \\
& [y_v, \hat{d}, \hat{e}, y_v], [y_v, \hat{e}, \hat{e}, y_v], [y_v, \hat{e}, \hat{f}, y_w], [y_u, y_v, y_w, y_w], [y_u, y_w, y_v, y_v], \\
& [y_u, y_w, y_w, y_w], [y_v, y_v, y_w, y_w], [y_v, y_w, y_v, y_v], [y_v, y_w, y_w, y_w], [y_w, y_w, y_u, y_u]. \quad (10.1)
\end{aligned}$$

Then the only nonvanishing quadruple at $(1, 0, 0)$ is $[\hat{f}, y_w, \hat{e}, y_v]$, and this is true for the weight 12, 14 and 16 Z functions.

For example, the relevant quadruple coproduct of the suitably normalized weight 12 Z function is

$$\begin{aligned}
Z_{\text{wt. 12}}^{\hat{f}, y_w, \hat{e}, y_v}(1, 0, 0) &= -\frac{1}{576} \ln^4 \hat{v} \ln^4 \hat{w} - \frac{\zeta_2}{48} \ln^2 \hat{v} \ln^2 \hat{w} (\ln^2 \hat{v} + \ln^2 \hat{w}) \\
&+ \frac{5}{96} \zeta_4 (\ln^4 \hat{v} + \ln^4 \hat{w} - 12 \ln^2 \hat{v} \ln^2 \hat{w}) + \left[\frac{35}{32} \zeta_6 - (\zeta_3)^2 \right] (\ln^2 \hat{v} + \ln^2 \hat{w}) \\
&- \frac{175}{96} \zeta_8 + 8 \zeta_3 \zeta_5 - 4 \zeta_2 (\zeta_3)^2, \quad (10.2)
\end{aligned}$$

which contains no irreducible MZV; i.e. no $\zeta_{5,3}$. The quadruples $Z_{\text{wt. } 14}^{\hat{f}, y_w, \hat{e}, y_v}$ and $Z_{\text{wt. } 16}^{\hat{f}, y_w, \hat{e}, y_v}$ also contain no irreducible MZVs at weight 10 and 12, respectively. (Lower-weight irreducible MZVs could also appear in principle, multiplied by $\ln \hat{v}$ and/or $\ln \hat{w}$, but they do not.)

Similarly, very few of the 70 independent quintuples are nonvanishing at $(1, 0, 0)$. With the basis we use, only four quintuples are nonvanishing, and three of them are always identical to each other:

$$Z^{\hat{e}, y_w, y_w, y_u, y_u} ; \quad Z^{\hat{f}, \hat{d}, y_v, \hat{f}, y_w} = Z^{\hat{f}, y_v, \hat{d}, \hat{e}, y_v} = Z^{\hat{f}, y_v, \hat{e}, \hat{f}, y_w} \quad (10.3)$$

None of these quantities contain irreducible MZVs either. We worked out the hextuples at $(1, 0, 0)$ as well, for the weight 14 and weight 16 Z functions for which they have weights 8 and 10, respectively, and we found no irreducible MZVs. Since there are no irreducible MZVs below weight 8, that completes the search for the weight 12 and 14 Z functions, and makes it implausible that there are any for weight 16 either. The conclusion is that the Z functions seem to be genuine function-level ambiguities in \mathcal{H}^{hex} , for lifting off of the $\Delta = 0$ surface.

10.2 Behavior at the origin

As mentioned earlier, one of the dihedrally symmetric weight 16 Z functions vanishes at the origin at symbol level. However, it is non-vanishing at function level. In fact all of the weight 16 Z function ambiguities can be fixed using only coefficients of $\ln^k u$ for $k = 4, 6, 8$. This statement is consistent with our earlier analysis, where the higher-weight constants were all fixed by consistency between the $(1, \hat{v}, \hat{v})$ and $(\hat{u}, 0, 0)$ lines, before ever going to the origin. Again, it means that the 8-loop value at the origin (5.1) is a pure cross check. Interestingly, the maximal degree of the Z functions in any individual $\ln \hat{u}_i$ at the origin is equal to the weight minus 8; i.e. degree 4 at weight 12, degree 6 at weight 14, and degree 8 at weight 16. In fact, on the entire line $(\hat{u}, 0, 0)$, the Z functions have this same maximal degree in $\ln \hat{v}$ and in $\ln \hat{w}$. In the ancillary file `Zorigin.txt`, we give the behavior at the origin for the 9 true weight 16 Z functions, as well as the tenth which is ζ_4 times the weight 12 Z function.

10.3 Fixing the last weight 11 constants

Refs. [26, 31] gave a description of hexagon functions through weight 11. At weight 11, however, there were six missing constants, n_i , $i = 1, 2, \dots, 6$, associated with the constant values of the hexagon functions at the reference point $(\hat{u}, \hat{v}, \hat{w}) = (1, 1, 1)$ that were provided in the ancillary file `SixGluonAmpsAndCops`. The six n_i were expected to be integers, but there was not enough information to fix them all at that stage.

In the process of integrating up the full eight-loop MHV function, consistency conditions on the integration completely fix all but one of these constants. (In contrast, the seven-loop NMHV amplitude [28] still leaves some of the six constants unfixed.) The final constant can be fixed by examining the weight 16 ambiguity functions and requiring the following branch-cut condition to hold,

$$Z_{\text{wt. } 16}^{y_v, x_1, x_2, x_3, x_4}(1, 0, 0) = Z_{\text{wt. } 16}^{y_w, x_1, x_2, x_3, x_4}(1, 0, 0) = 0, \quad (10.4)$$

for any letters x_i . The resulting values of the n_i are all indeed integers,

$$\begin{aligned} n_1 &= -337920, & n_2 &= -16896, & n_3 &= -608256, \\ n_4 &= 236544, & n_5 &= -1317888, & n_6 &= 9934848. \end{aligned} \tag{10.5}$$

This result completes the specification of the hexagon function space \mathcal{H}^{hex} through weight 11. As seen in section 8, we now know that a bit fewer functions are actually required, but at least their behavior is now totally determined.

11 The lines $(\hat{u}, \hat{u}, 1)$ and $(\hat{u}, 1, 1)$

The L -loop MHV amplitudes are very complicated for general $(\hat{u}, \hat{v}, \hat{w})$, but they simplify drastically on two lines, where we will plot them. On the lines $(\hat{u}, \hat{v}, \hat{w}) = (\hat{u}, \hat{u}, 1)$ and $(\hat{u}, \hat{v}, \hat{w}) = (\hat{u}, 1, 1)$, the hexagon symbol alphabet \mathcal{L}_{hex} collapses to just two letters, $\{\hat{u}, 1 - \hat{u}\}$. All hexagon functions become HPLs [4] $H_{\vec{a}}(1 - \hat{u})$, with $a_i \in \{0, 1\}$. By dihedral symmetry, it is enough to provide and plot $\mathcal{E}(\hat{u}, \hat{u}, 1)$ and $\mathcal{E}(\hat{u}, 1, 1)$. In the ancillary files `EZMHVg_uu1_lin.txt` and `EZMHVg_u11_lin.txt`, we provide these functions through eight loops, in four different linearized HPL representations, which can be used to series expand around the points $\hat{u} = 0, 1, \infty$. (Results in the old normalization through seven loops were provided in the ancillary file `SixGluonHPLLines.m` for refs. [26, 31].) These series expansions have overlapping regions of convergence, which makes it possible to plot the amplitudes on the full lines.

Before moving outward on the two lines, we discuss the behavior at two points. The first point is the Euclidean base point $(1, 1, 1)$ which lies at the intersection of the two lines. The analytical value is given in eq. (9.14), and the blue coefficients are predicted by antipodal duality from the eight-loop form factor, by reversing the order of the indices of the f 's. The numerical value of the eight-loop amplitude at that point is

$$\mathcal{E}^{(8)}(1, 1, 1) = -47748904.85576496624997891660892743663\dots \tag{11.1}$$

In Table 5 we give the numerical values of $\mathcal{E}^{(L)}(1, 1, 1)$ through $L = 8$ loops, as well as ratios of successive loop orders, which appear to tend toward the ratio -16 obeyed by the cusp anomalous dimension [65], $\Gamma_{\text{cusp}}^{(L)}/\Gamma_{\text{cusp}}^{(L-1)} \rightarrow -16$ as $L \rightarrow \infty$. In Table 6 we provide the values of the successive loop-order ratios for the remainder function at $(1, 1, 1)$. This ratio approaches -16 somewhat faster than the one for \mathcal{E} .

The second point we discuss is the limit as $\hat{u} \rightarrow \infty$ along the line $(\hat{u}, \hat{u}, 1)$, or $(\infty, \infty, 1)$ for short. Values at this point, like at $(1, 1, 1)$ are MZVs, and antipodal duality relates this point to the form factor at the point $(u, v) = (1, +\infty)$, i.e. the limit $v \rightarrow \infty$ of the line $u = 1$.

L	$\mathcal{E}^{(L)}(1, 1, 1)$	$\mathcal{E}^{(L)}(1, 1, 1)/\mathcal{E}^{(L-1)}(1, 1, 1)$
1	0	–
2	–9.740909108	–
3	123.0985106	–12.63727124
4	–1508.319856	–12.25294968
5	19196.41479	–12.72701855
6	–253379.3991	–13.19930841
7	3440841.652	–13.57980035
8	–47748904.85	–13.87710034

Table 5: The value of the L -loop MHV amplitude at $(\hat{u}, \hat{v}, \hat{w}) = (1, 1, 1)$ through eight loops, in the new cosmic normalization, and the ratio to the previous loop order.

L	$\mathcal{R}^{(L)}(1, 1, 1)$	$\mathcal{R}^{(L)}(1, 1, 1)/\mathcal{R}^{(L-1)}(1, 1, 1)$
2	–10.823232337111	–
3	151.61375458732	–14.00817702
4	–1997.6785778253	–13.17610386
5	26805.799395885	–13.41847467
6	–368506.63803885	–13.74727284
7	5169794.4229268	–14.02904015
8	–73696028.745912	–14.25511784

Table 6: MHV remainder function and successive loop order ratios at $(1, 1, 1)$ through eight loops.

The value is

$$\begin{aligned}
\mathcal{E}^{(8)}(\infty, \infty, 1) = & -\frac{5259063125}{18} f_{9,7} - \frac{40774437223}{144} f_{7,9} - \frac{49527178109}{120} f_{11,5} \\
& - \frac{76882560437}{240} f_{5,11} - \frac{589315976143}{1680} f_{13,3} - \frac{3806228668547}{16800} f_{3,13} \\
& - 19525796 f_{5,5,3,3} - 19216724 f_{5,3,5,3} - 21675228 f_{5,3,3,5} - 13812532 f_{3,5,5,3} \\
& - 15382068 f_{3,5,3,5} - 15703712 f_{3,3,5,5} - 20001939 f_{7,3,3,3} - 12334055 f_{3,7,3,3} \\
& - 12638203 f_{3,3,7,3} - 13916245 f_{3,3,3,7}
\end{aligned}$$

$$\begin{aligned}
& -\zeta_2 \left(\frac{5163836129}{16} f_{7,7} + \frac{2956391617}{9} f_{9,5} + \frac{5638517153}{18} f_{5,9} + \frac{49275366491}{120} f_{11,3} \right. \\
& \quad + \frac{54190442797}{240} f_{3,11} + 21672656 f_{5,3,3,3} + 14950352 f_{3,5,3,3} \\
& \quad \left. + 15412504 f_{3,3,5,3} + 15167512 f_{3,3,3,5} \right) \\
& -\zeta_4 \left(417940090 f_{7,5} + \frac{799758063}{2} f_{5,7} + 384992568 f_{9,3} + \frac{5187282665}{18} f_{3,9} \right. \\
& \quad \left. + 21691976 f_{3,3,3,3} \right) \\
& -\zeta_6 \left(\frac{1608784821}{4} f_{5,5} + \frac{9165154933}{24} f_{7,3} + \frac{1126390233}{4} f_{3,7} \right) \\
& -\zeta_8 \left(\frac{11463894607}{30} f_{5,3} + \frac{53213485753}{180} f_{3,5} \right) - \frac{50699228086}{175} \zeta_{10} f_{3,3} \\
& - \frac{537331216774792288437829}{82584825523200} \zeta_{16}. \tag{11.2}
\end{aligned}$$

The coefficients in blue agree perfectly with the predictions of antipodal duality from the eight-loop form factor.

Note that *all* coefficients entering $\mathcal{E}^{(8)}(\infty, \infty, 1)$ are negative, whereas for $\mathcal{E}^{(8)}(1, 1, 1)$ in eq. (9.13) they are all positive for the pure f terms, but have opposite sign for all ζ_{2n} (π^{2n}) terms except one. Remarkably, these sign patterns are also true at all lower loops (with no exceptions), after multiplying by an overall sign for odd loops. (See the ancillary file `AntipodePointsSummary.txt` for ref. [53] for the lower loop formulae.)

Next, we plot $\mathcal{E}(\hat{u}, \hat{u}, 1)$ in figure 2(a) through eight loops, as ratios of successive loop orders. For \hat{u} between 10^{-2} and 10^2 , remarkably, the ratios flatten out more and more with each additional loop, and they appear to be steadily approaching the cusp asymptotic ratio of -16 . There is a dip/spike feature in all the plots, simply because each function crosses zero at a slightly different value of \hat{u} . For $\hat{u} \rightarrow 0$ and $\hat{u} \rightarrow \infty$, the ratios no longer display the expected radius of convergence, either diverging logarithmically at different rates (for $\hat{u} \rightarrow 0$) or approaching constant values (as $\hat{u} \rightarrow \infty$) that do not have the same ratio of -16 between loop orders.

We plot the remainder function ratios $\mathcal{R}^{(L)}(\hat{u}, \hat{u}, 1)/\mathcal{R}^{(L-1)}(\hat{u}, \hat{u}, 1)$ on the same line in figure 2(b). These ratios do not exhibit the same degree of flattening in \hat{u} as the ratios $\mathcal{E}^{(L)}(\hat{u}, \hat{u}, 1)/\mathcal{E}^{(L-1)}(\hat{u}, \hat{u}, 1)$.

Now we turn to the line $(\hat{u}, 1, 1)$, which leaves the $\Delta = 0$ surface. We plot $\mathcal{E}(\hat{u}, 1, 1)$ in figure 3(a) through eight loops, as ratios between successive loop orders, for $1 \leq \hat{u} \leq 1000$. There is a pretty striking flattening of the ratios for $1 \leq \hat{u} \leq 100$, again generally approaching the radius of convergence suggested by the cusp anomalous dimension. In figure 3(b) the same ratio is plotted for the remainder function; as was the case for the line $(\hat{u}, \hat{u}, 1)$, the flattening is much less pronounced for the remainder function.

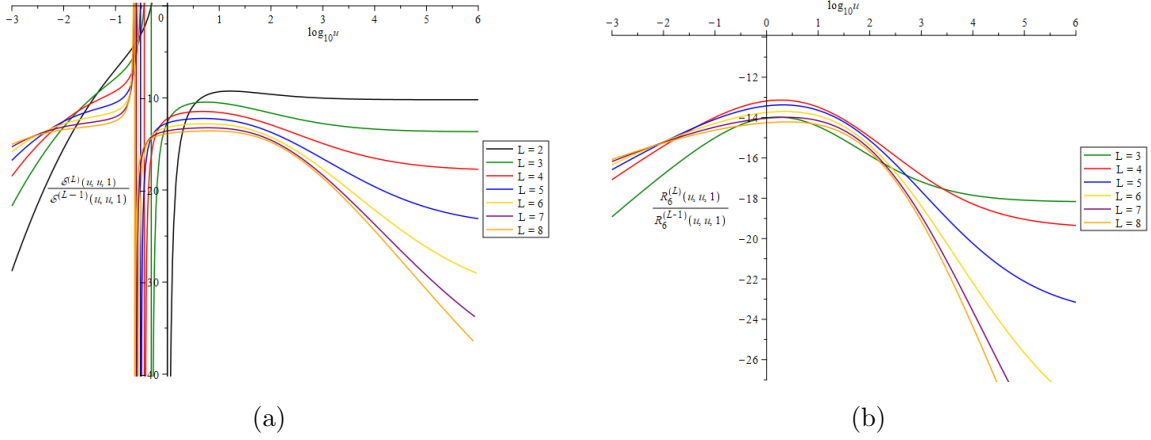


Figure 2: (a) $\mathcal{E}^{(L)}(\hat{u}, \hat{u}, 1)/\mathcal{E}^{(L-1)}(\hat{u}, \hat{u}, 1)$ evaluated at successive loop orders $L-1$ and L . As there are points where $\mathcal{E}^{(L)}(\hat{u}, \hat{u}, 1) = 0$ in this interval, the plot has many dip/spike features. (b) $\mathcal{R}^{(L)}(\hat{u}, \hat{u}, 1)/\mathcal{R}^{(L-1)}(\hat{u}, \hat{u}, 1)$ evaluated at successive loop orders.

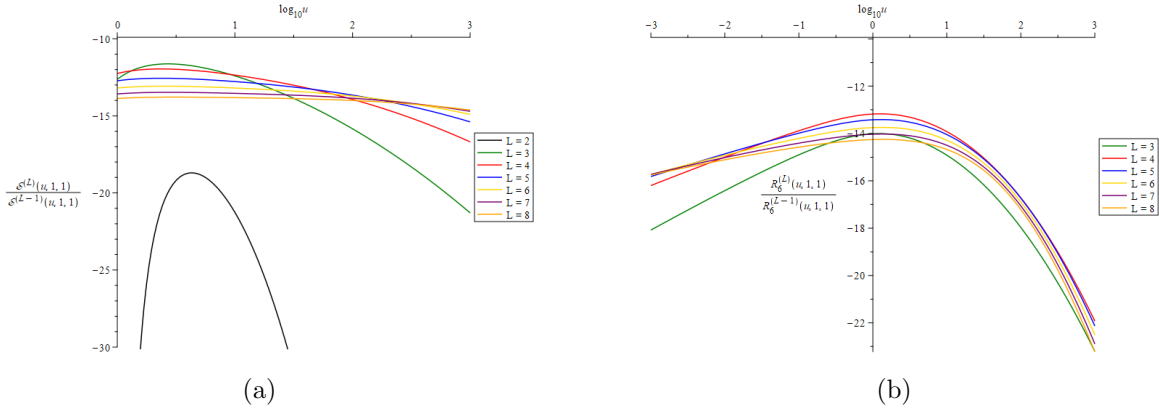


Figure 3: (a) The ratio $\mathcal{E}^{(L)}(\hat{u}, 1, 1)/\mathcal{E}^{(L-1)}(\hat{u}, 1, 1)$ evaluated at successive loop orders, $L-1$ and L . (b) $\mathcal{R}^{(L)}(\hat{u}, 1, 1)/\mathcal{R}^{(L-1)}(\hat{u}, 1, 1)$ evaluated at successive loop orders.

12 Conclusions

In this paper, we computed the eight-loop MHV six-particle amplitude in planar $\mathcal{N} = 4$ SYM, using the novel approach of determining it by assuming antipodal duality, and relying on the recently-computed [47] eight-loop three-point form factor of the chiral stress-energy tensor. This approach is also a bootstrap, making heavy use of the hexagon function space [26, 31], but the number of linear equations that have to be solved is far fewer with the form factor information. The number of equations that have to be solved at any one time could also be minimized by grading the quintuple final entries in the number of parity-odd y_i letters they contain. The amount of OPE information required was truly minimal, just enough to fix one beyond-the-symbol constant.

The fully fixed amplitude is in turn a rich source of information about the hexagon-function space, revealing additional final-entry relations, both in the bulk and at the base point $(1, 1, 1)$, as well as functions and constants that “drop out”, i.e. are not needed, particularly when the new cosmic normalization of the amplitude is employed. That there is a solution at all, and some of its beyond-the-symbol properties, is a validation of antipodal duality at eight loops.

The general idea of first fixing an amplitude or form factor on a suitable lower-dimensional surface, where the symbol alphabet simplifies, and then lifting it off the surface to full kinematics, should be applicable more broadly, even when antipodal duality is not there as a crutch. Parity-preserving surfaces also exist for higher-point amplitudes and form factors, and would be a natural place to try out such methods in the future.

Acknowledgments

We are grateful to Ömer Gürdoğan, Andrew McLeod and Matthias Wilhelm for collaboration on earlier related projects and for stimulating discussions. We also thank Benjamin Basso for useful conversations. This research was supported by the US Department of Energy under contracts DE-AC02-76SF00515 and DE-FOA-0002705, KA/OR55/22 (AIHEP), and by the Munich Institute for Astro-, Particle and BioPhysics (MIAPbP) which is funded by the Deutsche Forschungsgemeinschaft (DFG, German Research Foundation) under Germany’s Excellence Strategy – EXC-2094 – 390783311. LD thanks MIAPbP for hospitality during part of the writing of this paper.

References

- [1] K.-T. Chen, *Iterated path integrals*, *Bull. Amer. Math. Soc.* **83** (1977) 831.
- [2] A. B. Goncharov, *Geometry of configurations, polylogarithms, and motivic cohomology*, *Adv. Math.* **114** (1995) 197.
- [3] A. B. Goncharov, *Multiple polylogarithms, cyclotomy and modular complexes*, *Math. Res. Lett.* **5** (1998) 497 [[1105.2076](#)].
- [4] E. Remiddi and J. Vermaseren, *Harmonic polylogarithms*, *Int. J. Mod. Phys. A* **15** (2000) 725 [[hep-ph/9905237](#)].
- [5] J. M. Borwein, D. M. Bradley, D. J. Broadhurst and P. Lisonek, *Special values of multiple polylogarithms*, *Trans. Am. Math. Soc.* **353** (2001) 907 [[math/9910045](#)].
- [6] S. Moch, P. Uwer and S. Weinzierl, *Nested sums, expansion of transcendental functions and multiscale multiloop integrals*, *J.Math.Phys.* **43** (2002) 3363 [[hep-ph/0110083](#)].
- [7] A. B. Goncharov, M. Spradlin, C. Vergu and A. Volovich, *Classical Polylogarithms for Amplitudes and Wilson Loops*, *Phys. Rev. Lett.* **105** (2010) 151605 [[1006.5703](#)].
- [8] J. M. Drummond, J. Henn, V. A. Smirnov and E. Sokatchev, *Magic identities for conformal four-point integrals*, *JHEP* **01** (2007) 064 [[hep-th/0607160](#)].

- [9] Z. Bern, M. Czakon, L. J. Dixon, D. A. Kosower and V. A. Smirnov, *The Four-Loop Planar Amplitude and Cusp Anomalous Dimension in Maximally Supersymmetric Yang-Mills Theory*, *Phys. Rev.* **D75** (2007) 085010 [[hep-th/0610248](#)].
- [10] Z. Bern, J. Carrasco, H. Johansson and D. Kosower, *Maximally supersymmetric planar Yang-Mills amplitudes at five loops*, *Phys.Rev.* **D76** (2007) 125020 [[0705.1864](#)].
- [11] L. F. Alday and J. M. Maldacena, *Gluon scattering amplitudes at strong coupling*, *JHEP* **06** (2007) 064 [[0705.0303](#)].
- [12] J. M. Drummond, J. Henn, G. P. Korchemsky and E. Sokatchev, *Dual superconformal symmetry of scattering amplitudes in $\mathcal{N} = 4$ super-Yang-Mills theory*, *Nucl. Phys.* **B828** (2010) 317 [[0807.1095](#)].
- [13] Z. Bern, L. J. Dixon, D. A. Kosower, R. Roiban, M. Spradlin, C. Vergu et al., *The Two-Loop Six-Gluon MHV Amplitude in Maximally Supersymmetric Yang-Mills Theory*, *Phys. Rev.* **D78** (2008) 045007 [[0803.1465](#)].
- [14] J. Drummond, J. Henn, G. Korchemsky and E. Sokatchev, *Hexagon Wilson loop = six-gluon MHV amplitude*, *Nucl.Phys.* **B815** (2009) 142 [[0803.1466](#)].
- [15] V. Del Duca, C. Duhr and V. A. Smirnov, *An Analytic Result for the Two-Loop Hexagon Wilson Loop in $N = 4$ SYM*, *JHEP* **03** (2010) 099 [[0911.5332](#)].
- [16] V. Del Duca, C. Duhr and V. A. Smirnov, *The Two-Loop Hexagon Wilson Loop in $N = 4$ SYM*, *JHEP* **05** (2010) 084 [[1003.1702](#)].
- [17] J. Golden, A. B. Goncharov, M. Spradlin, C. Vergu and A. Volovich, *Motivic Amplitudes and Cluster Coordinates*, *JHEP* **1401** (2014) 091 [[1305.1617](#)].
- [18] J. Golden and M. Spradlin, *A Cluster Bootstrap for Two-Loop MHV Amplitudes*, *JHEP* **02** (2015) 002 [[1411.3289](#)].
- [19] L. J. Dixon, J. M. Drummond and J. M. Henn, *Bootstrapping the three-loop hexagon*, *JHEP* **1111** (2011) 023 [[1108.4461](#)].
- [20] L. J. Dixon, J. M. Drummond and J. M. Henn, *Analytic result for the two-loop six-point NMHV amplitude in $\mathcal{N} = 4$ super Yang-Mills theory*, *JHEP* **1201** (2012) 024 [[1111.1704](#)].
- [21] L. J. Dixon, J. M. Drummond, M. von Hippel and J. Pennington, *Hexagon functions and the three-loop remainder function*, *JHEP* **1312** (2013) 049 [[1308.2276](#)].
- [22] L. J. Dixon and M. von Hippel, *Bootstrapping an NMHV amplitude through three loops*, *JHEP* **1410** (2014) 65 [[1408.1505](#)].
- [23] L. J. Dixon, J. M. Drummond, C. Duhr and J. Pennington, *The four-loop remainder function and multi-Regge behavior at NNLLA in planar $\mathcal{N} = 4$ super-Yang-Mills theory*, *JHEP* **1406** (2014) 116 [[1402.3300](#)].
- [24] L. J. Dixon, M. von Hippel and A. J. McLeod, *The four-loop six-gluon NMHV ratio function*, *JHEP* **01** (2016) 053 [[1509.08127](#)].
- [25] S. Caron-Huot, L. J. Dixon, A. McLeod and M. von Hippel, *Bootstrapping a Five-Loop Amplitude Using Steinmann Relations*, *Phys. Rev. Lett.* **117** (2016) 241601 [[1609.00669](#)].

- [26] S. Caron-Huot, L. J. Dixon, F. Dulat, M. von Hippel, A. J. McLeod and G. Papathanasiou, *Six-Gluon amplitudes in planar $\mathcal{N} = 4$ super-Yang-Mills theory at six and seven loops*, *JHEP* **08** (2019) 016 [[1903.10890](#)].
- [27] S. Caron-Huot, L. J. Dixon, J. M. Drummond, F. Dulat, J. Foster, O. Gürdoğan et al., *The Steinmann Cluster Bootstrap for $\mathcal{N} = 4$ Super Yang-Mills Amplitudes*, *PoS CORFU2019* (2020) 003 [[2005.06735](#)].
- [28] L. Dixon and F. Dulat, “The Seven-Loop Six-Gluon NMHV Amplitude in Planar $\mathcal{N} = 4$ Super-Yang-Mills Theory.” to appear.
- [29] D. Gaiotto, J. Maldacena, A. Sever and P. Vieira, *Pulling the straps of polygons*, *JHEP* **12** (2011) 011 [[1102.0062](#)].
- [30] S. Caron-Huot, L. J. Dixon, M. von Hippel, A. J. McLeod and G. Papathanasiou, *The Double Pentagonal Integral to All Orders*, *JHEP* **07** (2018) 170 [[1806.01361](#)].
- [31] S. Caron-Huot, L. J. Dixon, F. Dulat, M. Von Hippel, A. J. McLeod and G. Papathanasiou, *The Cosmic Galois Group and Extended Steinmann Relations for Planar $\mathcal{N} = 4$ SYM Amplitudes*, *JHEP* **09** (2019) 061 [[1906.07116](#)].
- [32] S. He, Z. Li and Q. Yang, *Comments on all-loop constraints for scattering amplitudes and Feynman integrals*, *JHEP* **01** (2022) 073 [[2108.07959](#)].
- [33] J. Drummond, J. Foster and Ö. Gürdoğan, *Cluster Adjacency Properties of Scattering Amplitudes in $\mathcal{N} = 4$ Supersymmetric Yang-Mills Theory*, *Phys. Rev. Lett.* **120** (2018) 161601 [[1710.10953](#)].
- [34] J. Drummond, J. Foster, Ö. Gürdoğan and G. Papathanasiou, *Cluster adjacency and the four-loop NMHV heptagon*, *JHEP* **03** (2019) 087 [[1812.04640](#)].
- [35] L. F. Alday, D. Gaiotto, J. Maldacena, A. Sever and P. Vieira, *An Operator Product Expansion for Polygonal null Wilson Loops*, *JHEP* **1104** (2011) 088 [[1006.2788](#)].
- [36] B. Basso, A. Sever and P. Vieira, *Spacetime and Flux Tube S-Matrices at Finite Coupling for $\mathcal{N} = 4$ Supersymmetric Yang-Mills Theory*, *Phys. Rev. Lett.* **111** (2013) 091602 [[1303.1396](#)].
- [37] B. Basso, A. Sever and P. Vieira, *Space-time S-matrix and Flux tube S-matrix II. Extracting and Matching Data*, *JHEP* **1401** (2014) 008 [[1306.2058](#)].
- [38] B. Basso, A. Sever and P. Vieira, *Space-time S-matrix and Flux-tube S-matrix III. The two-particle contributions*, *JHEP* **08** (2014) 085 [[1402.3307](#)].
- [39] J. Drummond, G. Korchemsky and E. Sokatchev, *Conformal properties of four-gluon planar amplitudes and Wilson loops*, *Nucl. Phys. B* **795** (2008) 385 [[0707.0243](#)].
- [40] A. Brandhuber, P. Heslop and G. Travaglini, *MHV amplitudes in $\mathcal{N} = 4$ super Yang-Mills and Wilson loops*, *Nucl. Phys. B* **794** (2008) 231 [[0707.1153](#)].
- [41] L. F. Alday and J. Maldacena, *Comments on gluon scattering amplitudes via AdS/CFT*, *JHEP* **0711** (2007) 068 [[0710.1060](#)].
- [42] J. Drummond, J. Henn, G. Korchemsky and E. Sokatchev, *Conformal Ward identities for Wilson loops and a test of the duality with gluon amplitudes*, *Nucl.Phys.* **B826** (2010) 337 [[0712.1223](#)].

- [43] L. F. Alday and R. Roiban, *Scattering Amplitudes, Wilson Loops and the String/Gauge Theory Correspondence*, *Phys. Rept.* **468** (2008) 153 [[0807.1889](#)].
- [44] T. Adamo, M. Bullimore, L. Mason and D. Skinner, *Scattering Amplitudes and Wilson Loops in Twistor Space*, *J. Phys. A* **44** (2011) 454008 [[1104.2890](#)].
- [45] R. Ben-Israel, A. G. Tumanov and A. Sever, *Scattering amplitudes — Wilson loops duality for the first non-planar correction*, *JHEP* **08** (2018) 122 [[1802.09395](#)].
- [46] L. J. Dixon, A. J. McLeod and M. Wilhelm, *A Three-Point Form Factor Through Five Loops*, *JHEP* **04** (2021) 147 [[2012.12286](#)].
- [47] L. J. Dixon, O. Gürdoğan, A. J. McLeod and M. Wilhelm, *Bootstrapping a stress-tensor form factor through eight loops*, *JHEP* **07** (2022) 153 [[2204.11901](#)].
- [48] A. Brandhuber, B. Spence, G. Travaglini and G. Yang, *Form Factors in $\mathcal{N} = 4$ Super Yang-Mills and Periodic Wilson Loops*, *JHEP* **01** (2011) 134 [[1011.1899](#)].
- [49] A. Brandhuber, G. Travaglini and G. Yang, *Analytic two-loop form factors in $\mathcal{N} = 4$ SYM*, *JHEP* **05** (2012) 082 [[1201.4170](#)].
- [50] A. Sever, A. G. Tumanov and M. Wilhelm, *Operator Product Expansion for Form Factors*, *Phys. Rev. Lett.* **126** (2021) 031602 [[2009.11297](#)].
- [51] A. Sever, A. G. Tumanov and M. Wilhelm, *An Operator Product Expansion for Form Factors II. Born level*, *JHEP* **10** (2021) 071 [[2105.13367](#)].
- [52] A. Sever, A. G. Tumanov and M. Wilhelm, *An Operator Product Expansion for Form Factors III. Finite Coupling and Multi-Particle Contributions*, *JHEP* **03** (2022) 128 [[2112.10569](#)].
- [53] L. J. Dixon, Ö. Gürdoğan, A. J. McLeod and M. Wilhelm, *Folding Amplitudes into Form Factors: An Antipodal Duality*, *Phys. Rev. Lett.* **128** (2022) 111602 [[2112.06243](#)].
- [54] L. J. Dixon, O. Gürdoğan, Y.-T. Liu, A. J. McLeod and M. Wilhelm, *Antipodal Self-Duality for a Four-Particle Form Factor*, *Phys. Rev. Lett.* **130** (2023) 111601 [[2212.02410](#)].
- [55] L. J. Dixon, O. Gürdoğan, Y.-T. Liu, A. J. McLeod and M. Wilhelm, “More Antipodal Self-Duality.” to appear.
- [56] B. Basso, L. J. Dixon and G. Papathanasiou, *The Origin of the Six-Gluon Amplitude in Planar $\mathcal{N} = 4$ SYM*, *Phys. Rev. Lett.* **124** (2020) 161603 [[2001.05460](#)].
- [57] B. Basso, L. J. Dixon, Y.-T. Liu and G. Papathanasiou, *An Origin Story for Amplitudes*, *Phys. Rev. Lett.* **130** (2023) 111602 [[2211.12555](#)].
- [58] B. Basso, S. Caron-Huot and A. Sever, *Adjoint BFKL at finite coupling: a short-cut from the collinear limit*, *JHEP* **01** (2015) 027 [[1407.3766](#)].
- [59] <http://www.slac.stanford.edu/~lance/Cosmic/>.
- [60] A. B. Goncharov, *Galois symmetries of fundamental groupoids and noncommutative geometry*, *Duke Math. J.* **128** (2005) 209 [[math/0208144](#)].
- [61] F. Brown, *On the decomposition of motivic multiple zeta values*, *Adv. Studies in Pure Math.* **63** (2012) 31 [[1102.1310](#)].
- [62] C. Duhr, *Hopf algebras, coproducts and symbols: an application to Higgs boson amplitudes*, *JHEP* **1208** (2012) 043 [[1203.0454](#)].

- [63] F. Brown, *Mixed Tate motives over \mathbb{Z}* , *Ann. of Math. (2)* **175** (2012) 949 [[1102.1312](#)].
- [64] F. Brown, *Feynman amplitudes, coaction principle, and cosmic Galois group*, *Commun. Num. Theor. Phys.* **11** (2017) 453 [[1512.06409](#)].
- [65] N. Beisert, B. Eden and M. Staudacher, *Transcendentality and Crossing*, *J. Stat. Mech.* **0701** (2007) P01021 [[hep-th/0610251](#)].
- [66] V. Del Duca, S. Druc, J. Drummond, C. Duhr, F. Dulat, R. Marzucca et al., *Multi-Regge kinematics and the moduli space of Riemann spheres with marked points*, *JHEP* **08** (2016) 152 [[1606.08807](#)].
- [67] A. von Manteuffel and R. M. Schabinger, *A novel approach to integration by parts reduction*, *Phys. Lett. B* **744** (2015) 101 [[1406.4513](#)].
- [68] T. Peraro, *Scattering amplitudes over finite fields and multivariate functional reconstruction*, *JHEP* **12** (2016) 030 [[1608.01902](#)].
- [69] O. Schnetz. Computer program HYPERLOGPROCEDURES, <https://www.math.fau.de/person/oliver-schnetz/>.
- [70] L. J. Dixon and I. Esterlis, *All orders results for self-crossing Wilson loops mimicking double parton scattering*, *JHEP* **07** (2016) 116 [[1602.02107](#)].
- [71] G. Georgiou, *Null Wilson loops with a self-crossing and the Wilson loop/amplitude conjecture*, *JHEP* **09** (2009) 021 [[0904.4675](#)].
- [72] H. Dorn and S. Wuttke, *Wilson loop remainder function for null polygons in the limit of self-crossing*, *JHEP* **05** (2011) 114 [[1104.2469](#)].
- [73] H. Dorn and S. Wuttke, *Hexagon Remainder Function in the Limit of Self-Crossing up to three Loops*, *JHEP* **04** (2012) 023 [[1111.6815](#)].
- [74] S. Caron-Huot. private communication.
- [75] B. Basso, A. Sever and P. Vieira, *Collinear Limit of Scattering Amplitudes at Strong Coupling*, *Phys. Rev. Lett.* **113** (2014) 261604 [[1405.6350](#)].
- [76] B. Basso, A. Sever and P. Vieira, *Space-time S-matrix and Flux-tube S-matrix IV. Gluons and Fusion*, *JHEP* **09** (2014) 149 [[1407.1736](#)].
- [77] A. Belitsky, *Nonsinglet pentagons and NMHV amplitudes*, *Nucl. Phys. B* **896** (2015) 493 [[1407.2853](#)].
- [78] A. Belitsky, *Fermionic pentagons and NMHV hexagon*, *Nucl. Phys. B* **894** (2015) 108 [[1410.2534](#)].
- [79] B. Basso, J. Caetano, L. Cordova, A. Sever and P. Vieira, *OPE for all Helicity Amplitudes*, *JHEP* **08** (2015) 018 [[1412.1132](#)].
- [80] A. V. Belitsky, *On factorization of multiparticle pentagons*, *Nucl. Phys.* **B897** (2015) 346 [[1501.06860](#)].
- [81] B. Basso, J. Caetano, L. Cordova, A. Sever and P. Vieira, *OPE for all Helicity Amplitudes II. Form Factors and Data Analysis*, *JHEP* **12** (2015) 088 [[1508.02987](#)].
- [82] B. Basso, A. Sever and P. Vieira, *Hexagonal Wilson loops in planar $\mathcal{N} = 4$ SYM theory at finite coupling*, *J. Phys. A* **49** (2016) 41LT01 [[1508.03045](#)].

- [83] A. Belitsky, *Matrix pentagons*, *Nucl. Phys. B* **923** (2017) 588 [[1607.06555](#)].
- [84] J. Bartels, L. Lipatov and A. Sabio Vera, *BFKL Pomeron, Reggeized gluons and Bern-Dixon-Smirnov amplitudes*, *Phys.Rev.* **D80** (2009) 045002 [[0802.2065](#)].
- [85] J. Bartels, L. N. Lipatov and A. Sabio Vera, *$N=4$ supersymmetric Yang Mills scattering amplitudes at high energies: The Regge cut contribution*, *Eur. Phys. J. C* **65** (2010) 587 [[0807.0894](#)].
- [86] V. S. Fadin and L. N. Lipatov, *BFKL equation for the adjoint representation of the gauge group in the next-to-leading approximation at $N=4$ SUSY*, *Phys. Lett. B* **706** (2012) 470 [[1111.0782](#)].
- [87] F. C. Brown, *Single-valued multiple polylogarithms in one variable*, *C. R. Acad. Sci. Paris, Ser. I* **338** (2004) 527.
- [88] L. J. Dixon, C. Duhr and J. Pennington, *Single-valued harmonic polylogarithms and the multi-Regge limit*, *JHEP* **1210** (2012) 074 [[1207.0186](#)].
- [89] V. Del Duca and L. J. Dixon, *The SAGEX review on scattering amplitudes Chapter 15: The multi-Regge limit*, *J. Phys. A* **55** (2022) 443016 [[2203.13026](#)].
- [90] M. Bullimore and D. Skinner, *Descent Equations for Superamplitudes*, [1112.1056](#).
- [91] S. Caron-Huot and S. He, *Jumpstarting the All-Loop S-Matrix of Planar $\mathcal{N} = 4$ Super Yang-Mills*, *JHEP* **1207** (2012) 174 [[1112.1060](#)].
- [92] M. Deneufchâtel, G. H. E. Duchamp, V. H. N. Minh and A. I. Solomon, *Independence of hyperlogarithms over function fields via algebraic combinatorics*, [1101.4497](#).
- [93] C. Duhr, H. Gangl and J. R. Rhodes, *From polygons and symbols to polylogarithmic functions*, *JHEP* **10** (2012) 075 [[1110.0458](#)].
- [94] O. Schnetz, *Graphical functions and single-valued multiple polylogarithms*, *Commun. Num. Theor. Phys.* **08** (2014) 589 [[1302.6445](#)].
- [95] E. Panzer and O. Schnetz, *The Galois coaction on ϕ^4 periods*, *Commun. Num. Theor. Phys.* **11** (2017) 657 [[1603.04289](#)].